

A Brief Study on Adaptable, Flexible, Tunable, Traceable and Self-Sustainable Smart Optical Systems

Diptendu Mitra*, B.B.Bhowmik,
Department of Electronics and Communication Engineering,
Tripura University, India.
Email: diptendumitra11@gmail.com*

Abstract : In this paper a review on some of the most important works ranging from Frequency Offset Tracing, FOE(Frequency Offset Estimation) to Flexi-grid long haul optical systems has been done. With the growing demands for higher data speed and more data quantity it is required that the receiver for communication systems is very well equipped with the latest and upgraded new technologies where a filter is made intelligent enough to trace the frequency drift, estimate frequency and phase offset and accordingly adjust its central frequency and also reconfigure the essential bandwidth as per needed for any modulation format(i.e; format-transparent) and at any bit rate.

IndexTerms - Fragmentation and de-fragmentation, De-fragmentation techniques, Frequency Offset(FO), Flexi-grid, Frequency Offset Tracing, frequency offset drift, MAP, Intradyme, Homodyne, Heterodyne and Spectrum Sweep(Scan).

I. INTRODUCTION

With the advancement of science and technology the need for luxury and sophisticated products is ever-growing along with the demand for faster, survivable, more scalable and flexible bandwidth, more data carrying capable and more reliable network systems.

Flexi-grid is a breakthrough technology over *fixed-grid* that allows the network operator to maximize the capacity of network by matching the channel bandwidth with signal data rate. It uses Liquid Crystal on Silicon Technology to address carrier demand on bandwidth required in next generation optical network. Today's optical network uses channel spacing of about 50GHz & can support a speed of 100Gbps but for 400Gbps or more(~1Tbps)more channel spacing is required. In fixed-grid, channel spacing can't be varied but in flexi-grid channel spacing of 50GHz can be varied along any frequencies up to the upper frequency limit(say 200GHz).Flexi-grid technology is software configurable i.e; channel spacing can be varied dynamically according to specific requirements so more unused or available spectrum regions can be saved for other uses.

It can be deduced from[71]in SMF(Single Mode Fiber), bit rate is inversely proportional to transmission distance. Now say, there is a demand of 100Gbps total capacity which can be achieved by using 10 channels of each 10Gbps or 20 channels of each 5Gbps.But the 20 channels has more granularity, lesser prone to optical fiber nonlinearities and reduces system sensitivity to degradations[70],[39].Granularity can also be increased by increasing the bit rate at different rate for different channels of a fixed total capacity. Also for DWDM we can group different wavelength channels together and give each groups different bit rates.

Fragmentation of spectrum resources that reduces spectral efficiency and hampers proper utilization of available or unused spectrum resources(spaces)can happen when there are two constraints. One is due to continuity constraint and the other due to contiguity constraint. For instance, we know in light there are *seven* major colors with their respective central nominal frequencies(from high frequency to low frequency VIBGYOR=Violet Indigo Blue Green Yellow Orange Red).All these seven colors are continuous i.e; they have a smooth transition with infinite number of frequency components ranging from red to violet and all these seven colors are contiguous(adjacent) i.e; we can not randomly put one color among other colors. For instance, violet can't be placed in place of orange just before red,orange and red are adjacent to each other always.

The light's bandwidth had been divided in spectrum units, known as frequency slices for accommodating data traffic. Granularity in spectrum slot as per ITU-T 694.1 standard[64], was given 12.5 GHz because 1THz, 1.5THz, and 2THz light bandwidths had 80, 120, and 160 frequency slices[65],[70] respectively. Thus, by varying allocated frequency slices spectrum variability of the connections had been achieved.

Let us consider there are three links(L1,L2 and L3)[67] as depicted in figure 1 below.Each links has 12 *frequency slots*(windows) of equal sizes(say 12.5GHz) and *slices*i.e; channel frequency spacing(spacing between two successive central nominal frequencies which is also say 12.5GHz). There are two demands D1 and D2. The D1 demands 4 slots in these three links(L1,L2,L3) which can't be allocated even if unused frequency slots(spectrum resources) available in first two links(L1 and L2) because of continuity constraint i.e; different spectrum can't be allocated in same light path channels.And D2 demands 6 slots in third Link(L3) which can't be allocated because of contiguity constraint i.e; 6 contiguous(adjacent)slots are not available.

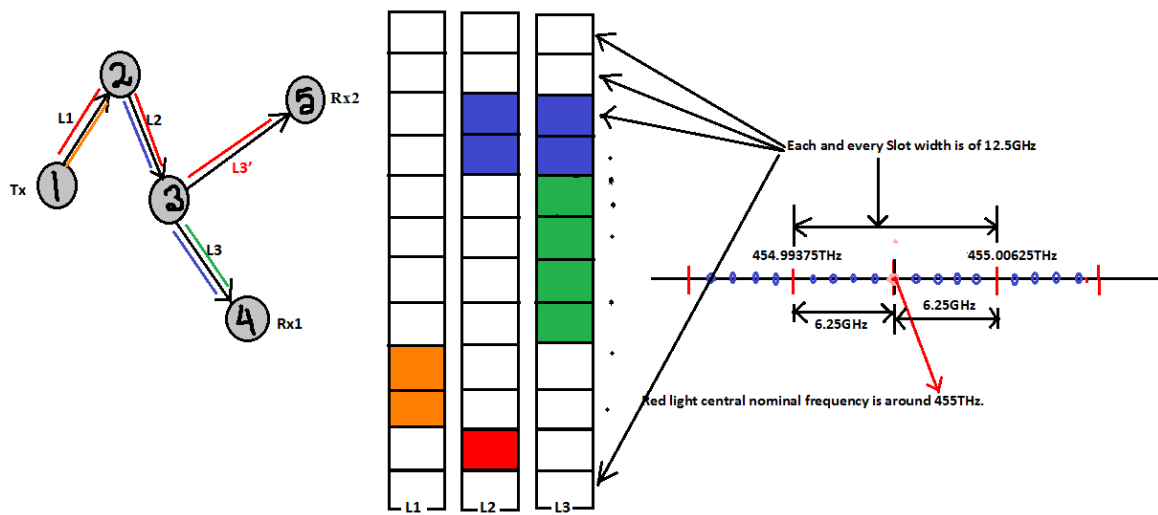


Figure: 1 Three links with 12 slots.[67]

(Red light has a range of ~700-635nm wavelength and ~430-480THz frequency.Redlight central nominal frequency is around 455THz.)

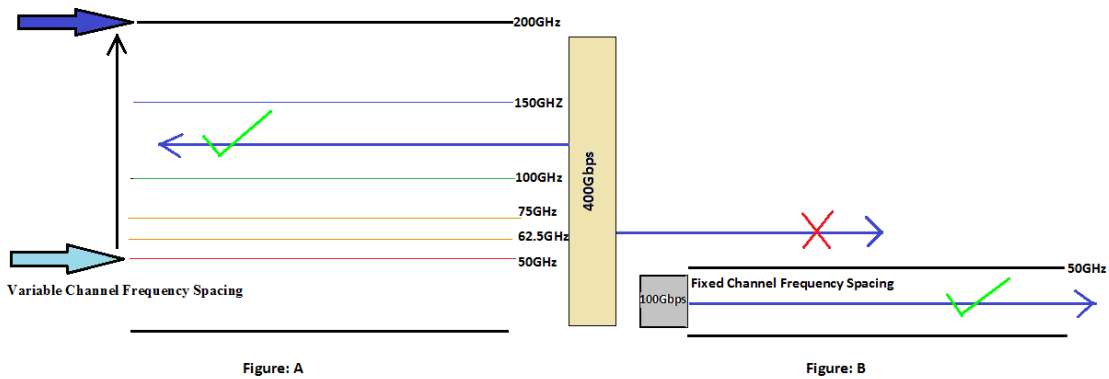


Figure 2:(A)Variable channel frequency spacing. Figure 2:(B) Fixed channel frequency spacing.[58],[65, P-34]

The latest technology advances provides us with the use of configurable region of light’s spectrum which has frequency slices(for instance, 12.5GHz slice). This slices had been customized to the needed channel bandwidth also known as *Slot Width*[28].There had been significant work done and still going on the Spectral Efficiency Optimization and Push-Pull defragmentation in Flexi-Grid Long-Haul Optical Systems without disruption in Data Traffic, Dynamic Bandwidth allocation and Flexible Wavelength for Ethernet Passive Optical Networks,

The Flexi-Grid also known as *Elastic Grid* technology relied on Bandwidth Variable Wavelength Selected Switches(BV-WSS)[28]used in DWDM optical communications networks to route (switch) signals between optical fibers on a per-wavelength basis.

II. LITERATURE REVIEW

In 2013, a work had been proposed on Push-Pull defragmentation by fellow authors, F.Cugini, F.Paolucci, G.Meloni, G.Berrettini, M.Secondini, F.Fresi,N.Sambo, L.Poti and P.Castoldi where they said that fragmentation of spectrum resources could significantly affect the efficiency of network. So effective and various defragmentation techniques had been proposed by the aforementioned authors[28] to curb the wasting of spectrum resources. The technique is called *Push-Pull* defragmentation. In their work, reconfiguration of allocated spectrum resources without traffic disruption by Dynamic Lightpath Frequency Retuning(DLFR) had been used.They didn’t use any additional transponders but they did use Bandwidth Variable Wavelength Selected Switches(BV-WSS)which came in very handy.The tuning of ECL Lasers and the control of filter bandwidth shaping with the help of BV-WSS were done using GMPLS(Generalized Multi-Protocol Label Switching). Push-Pull technique was first taken into account in flexible optical networks operated with light-paths that had On-Off Keying(OOK) modulation. It was used in direct modulation as well. They found there were limitations due to LASER technology & impairments. Push-Pull technique was then considered in flexible optical networks with lightpaths that had Advanced Modulation Formats. Modulation format includes for instance, Polarization Multiplexed Quadrature Phase shift Keying(PM-QPSK). Experimental demonstration for both direct & coherent detection had been done by them.

According to them, earlier for defragmentation MbB(Make-before-Break) technique was used where first a lightpath needed to be created between same source and destination nodes when a traffic disruption, connection loss etc. was detected .Then the traffic resources was switched from existing first connection to new connection of active network before breaking the original first connection. Although it had minimal to null traffic disruption but it required at least two expensive transponders at the source node as well as at the destination node. So, the Push-Pull defragmentation technique was born to mitigate all the existing issues of the optical network.

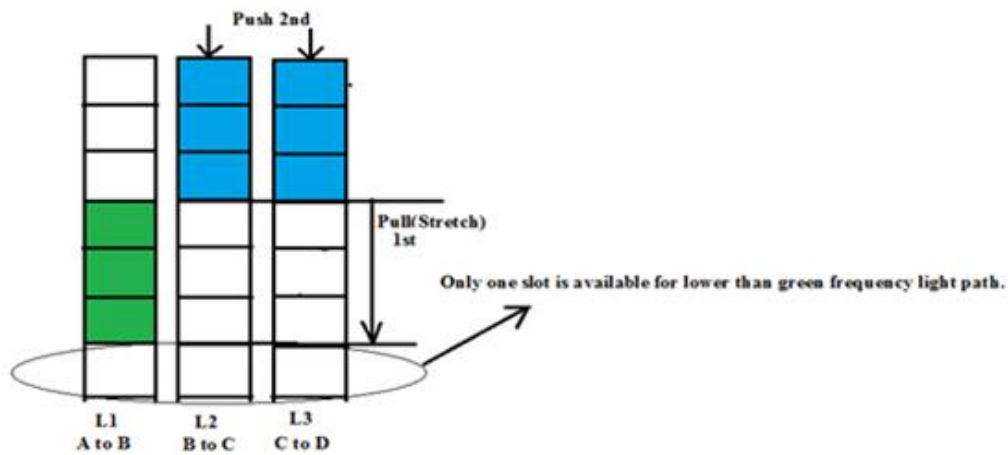
Push-Pull Technique:

As they described in their paper[28], Lightpaths from A to B and B to D have nominal central frequencies f_1 and f_2 respectively both with slot width of certain frequency slices. Although enough slices were available throughout, new lightpaths between A to D could not be established. For defragmenting the network resources, NMS(Network Management System)selects the lightpath B-D. Then B-D lightpath was tuned to f_1 as nominal central frequency from f_2 and thereby compressing the occupied spectrum resources neatly. Push-Pull defragmentation works in three steps:-

(i)They Dynamically Reconfigure the allocated spectrum resources, where a contiguous(adjacent) and unused spectrum along B-D was reserved. The spectrum was reserved such a way, for instance if 'x' frequency slices where 'x=3(say)' slices were available having f_1 central nominal frequency, this f_1 got included in the range of frequencies ($Y=2x$ slices for instance) allocated to original lightpath.

(ii)After that for instance, they first *stretched(pulled)* slot width of $x=3$ slots and then *pushed* f_2 towards f_1 by retuning of original lightpath's central nominal frequency from f_2 to f_1 and forced the receiver photodetector to operate at near f_1 central nominal frequency that shifted the top three slots of blue color in link 2 and 3 as in figure 3, all the way down to the lower three slots which are parallel to link 1 three green slots.

(iii)Further Dynamic Reconfiguration of allocated spectrum resources was done as in step (i).



Each and every 7 slots of three links is of 12.5GHz width

Figure: 3 Three links with 7 slots in push pull defragmentation.[28]



Figure:4 Push-Pull defragmentation in two links of three nodes A,B,C with 6slots and allocation of new light path(blue).[28]

While they were tuning the ECL laser by moving the central nominal frequency from one end to other, a frequency offset(FO) had been introduced between LO laser and transmitter ECL laser which they mitigated to an extent using AFC(Automatic Frequency control) algorithm. Different authors used different schemes and techniques to deal with this frequency offset issue and some schemes are discussed in this paper along with their pros and cons.

Comparison and discussion

For direct demodulation.

First reason for signal quality deterioration:

$$OSNR(\text{in dB}) = 10 \log_{10} \left(\frac{P_{avg.}}{P_{ASE}} \right) = 10 \log_{10} \left(\frac{\frac{P_{in}}{N_{in}}}{\frac{B_{resoln}}{B_{optical}}} \right) \dots (01) [45].$$

Here, $P_{avg.} = \frac{P_{in}}{N_{in}}$, average power. $P_{ASE} = \frac{B_{resoln}}{B_{optical}}$, Amplified

Spontaneous Emission power. P_{in} is input signal power. N_{in} is input noise power. B_{resoln} is bandwidth resolution. $B_{optical}$ is optical bandwidth.

Quality Factor Q can be written as:-

$$Q = \frac{2R(X-Z)P_{avg.}}{\sqrt{J_1 B_{electrical}} \left(\sqrt{X + \frac{J_2}{J_1}} + \sqrt{Z + \frac{J_2}{J_1}} \right)} \dots (02). [45].$$

Here, R=Responsivity (range is between 0 and 1). X and Z are upper and lower eye boundaries respectively. $J_1 = 4R(q + RS_{ASE})$. Here, S_{ASE} is power spectral density of ASE noise. And q is charge of electron ($1.6 \times 10^{-19}C$).

$$J_2 = S_{ASE} \cdot 2R^2(2B_{optical} - B_{electrical}). [45]$$

Here, $B_{electrical}$ is electrical receiver bandwidth.

$$\text{When ASE noise is dominating, } Q \approx \left(\frac{\sqrt{X}-\sqrt{Z}}{\sqrt{B_{electrical}}} \right) \times \frac{\sqrt{P_{avg.}}}{\sqrt{S_{ASE}}} = \left(\frac{\sqrt{X}-\sqrt{Z}}{\sqrt{B_{electrical}}} \right) \times \sqrt{OSNR} \dots (03). [45]$$

$$OSNR \text{ penalty } \delta = 10 \log_{10} \left(\frac{Q + \sqrt{2YT+1}}{Q + \sqrt{2xT+1}} \right) \dots (04) [28].$$

Here, T is bit duration time. And x is initial frequency slot. Y is stretched

$$\text{frequency slot. Also, } x \text{ can be the reference filter bandwidth. We know, } BER = \frac{1}{2} \text{erfc} \left(\frac{Q}{\sqrt{2}} \right) \approx \frac{1}{(\sqrt{2\pi})Q} e^{-\frac{Q^2}{2}} \dots (05) [45].$$

In their paper [28] they took negative logarithm of BER which gives, $-\log_{10}(BER) = \log_{10}(Q) + \log_{10}(\sqrt{2\pi}) + \frac{Q^2}{2} \log_{10}(e) = \log_{10}(Q) + 0.3991 + \frac{Q^2}{2} \times 0.4343 \dots (06). [45]$ Here, $e = 2.7183$.

From equation 02 and 04 during push-pull technique when bandwidth (slotwidth) is stretched and increased from x to $Y = k \times (x)$, $k = 2, 3, 4, \dots$ finite number etc. OSNR penalty is increased. Also from equation 02 and 03 optical bandwidth is increased that reduces Q quality factor and hence OSNR decreases. And so from equation 05 and 06 as Q quality factor decreases BER increases and

$-\log_{10}(BER)$ decreases with some slope. For stretched higher bandwidth this decreasing slope of $-\log_{10}(BER)$ is increased which BER is increased at faster rate.

It had been also found by them that for increasing filter bandwidth OSNR penalty is lesser and increasing at slower rate than theoretical OSNR penalty because filter narrowing effect [46] due to WSS that degrades the signal OSNR and Q quality factor was not considered in the equation 04. This is a disadvantage of the equation 04. In addition, OSNR penalty in OOK system was found to be increasing at higher rate with respect to OSNR penalty in PM-QPSK system.

Second reason for signal quality deterioration:

Unreduced residual chromatic dispersion as a result of time shift of data stream at the receiver end i.e; the incoming received signal baud rate (information rate) is slightly changed (ΔB) from transmitted signal baud rate.

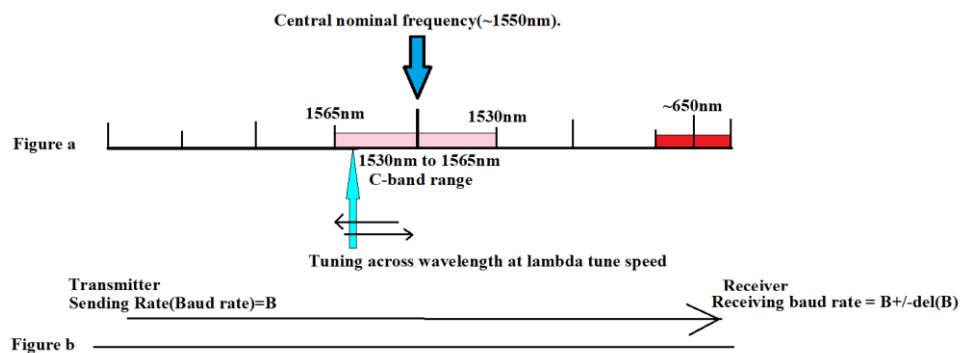


Figure: 5(a) Tuning across entire wavelength range of a tunable laser and especially nano (fine) tuning across C-band. (b) Change in information rate (baud rate B) at the receiver end. [28]

1530nm to 1565nm is (Conventional) C-band range. Central nominal frequency (~1550nm). Tuning across wavelength at λ_{Tune} speed. Transmitter Receiver Sending Rate (Baud rate) = B. Change in baud rate = (ΔB) . Receiving baud rate = $B \pm \Delta B$. Usually, from dispersion equation $D = -\left(\frac{2\pi c}{\lambda^2}\right) \beta_2$ when wavelength (λ) changing during tuning, D is changing hence chromatic dispersion D changing and that changes the baud rate by say $-\Delta B$. Practical laser tuning time across whole spectrum is greater than simply nano (fine) tuning across a portion of spectrum i.e; C-band (tuning across C-band is about in range of 1 to 10ms).

Pull out range of clock and data recovery $R_{pull-out} \geq |\Delta B| = \lambda_{Tune} \times l$. Here, l is dispersion length. It means, if receiver clock and data time after digital processing from received optical analog data from the time of sending at transmitter is less than $1/|\Delta B|$ dispersion time, then dispersion is somewhat avoided. For coherent demodulation:-

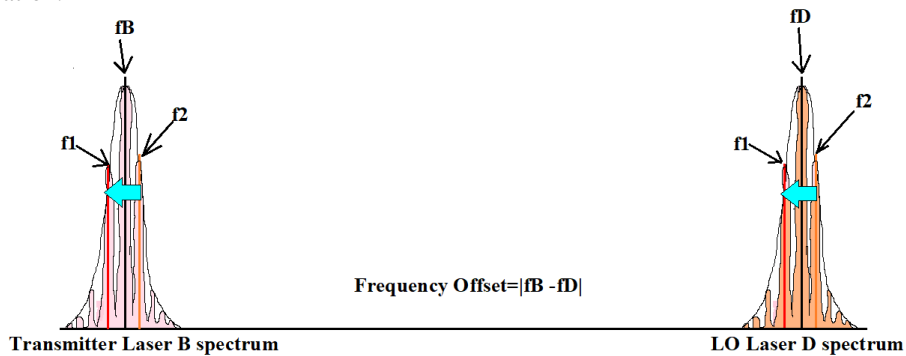


Figure: 6 Transmitter Laser B spectrum and LO Laser D spectrum where D follows B and f_2 tuned to f_1 and Frequency Offset(FO) = $|f_B - f_D|$. [28]

From figure: 3 and 6, laser B had wider frequency band(wavelength band). It is transmitting message signal with various carrier frequencies. Initial carrier frequency was f_2 for both transmitter end laser B and receiver end laser D. So before tuning actual central frequencies were $f_B \approx f_D \approx f_2$. Then f_B was pushed from f_2 to f_1 by transmitter laser nano(fine) tuning at tuning rate of $TR = \frac{df_B}{dt}$.

Frequency(wavelength) Tuning, frequency offset estimation and reduction of frequency offset was done automatically by a controller. A feedback loop was used so that frequency offset does not go beyond its maximum range. And they made the set up such that the receiver end laser D frequency f_D follows transmitter end laser B frequency f_B .

In their experiment at the start, transmitter laser frequency was tuned at $\lambda_{Tune} = 80\text{nm/s}$ speed from f_2 to f_1 while LO Laser frequency was fixed. That actually gave total frequency offset FO of 50GHz during data processing. This FO was reduced in steps of $\delta f = 1.25\text{GHz}$ to zero FO, after passing the signal through a loop 40 times repeatedly ($40 \times 1.25\text{GHz} = 50\text{GHz}$). f_B was heterodyned with f_{LO} for down conversion and also for getting very fine (small) frequency offset $\delta f = |f_B - f_{LO}|$.

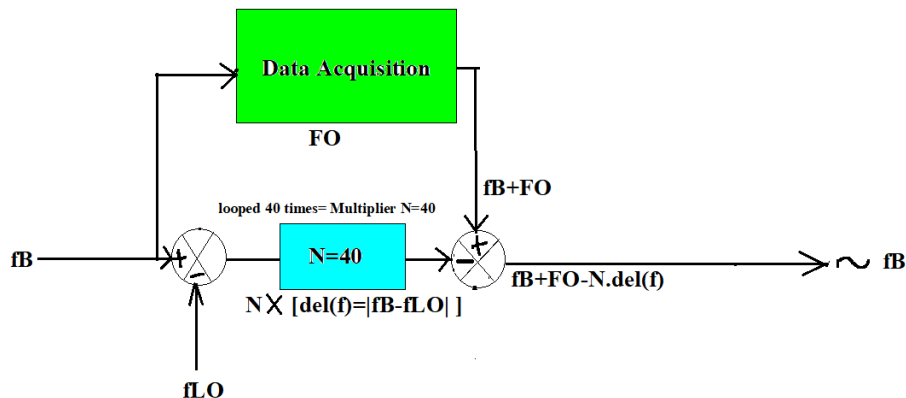


Figure: 7 Reduction of total frequency offset. [28]

To their surprise they found that with the increment of tuning speed, FO was increasing and as FO was increasing consequently BER was increasing. And for a particular forgetting factor $\alpha = 0.999$, MSE (Mean Square Error) increased by 0.0250. They found if α is reduced MSE can be reduced.

In 2015 there was a work done on spectral efficiency improvement by Tommasofoggi, Giulio Colavolpe, Alberto Bononi, Paolo Serena all members of IEEE. As we have read earlier Flexible-Grid optical Network provided with better utilization of fiber capacity through denser frequency allocation. Narrow filters were required in dense and tightly packed channel spacing and as a result of which linear ISI (Inter Symbol Interference) that got increased may dramatically reduce the transmission distance. In their paper they showed that by including a simple trellis processing at the receiver end, along with information theory techniques that was used in DWDM and Nyquist-WDM to take care of linear ISI (Inter Symbol Interference), maintaining a good quality SE (Spectral Efficiency) and optimum transmission distance was somewhat possible.

In their simulated WDM system, linearly modulated N_c , randomly polarized PM signals were launched after random detuning of central nominal frequency.

They had considered a QPSK modulation format throughout the whole. The transmitted signal's complex envelope on i -th polarization and l -th carrier was given by them as:

$$X = \sum_{k=0}^{K-1} x_k^{(i,l)} p(t - kT - \tau^{(i,l)}) e^{j[2\pi l(F + \Delta f)t + \theta^{(i,l)}]} \quad (07)[29]$$

where, $p(t)$ = shaping pulse with RRC(Root Raised Cosine)spectrum with roll-off factor $\alpha = 0.1$, K number of symbols were transmitted on each and every carrier. And those K symbols were transmitted also on each polarization. T was the symbol duration, $x_k^{(i,l)}$ is symbol transmitted during kth symbol interval, $\tau^{(i,l)}$ is delay, $\theta^{(i,l)}$ is initial phase of i-th polarization and l-th carrier. F is frequency spacing between two adjacent carriers. And Δf is frequency offset ($\Delta f \ll F$).

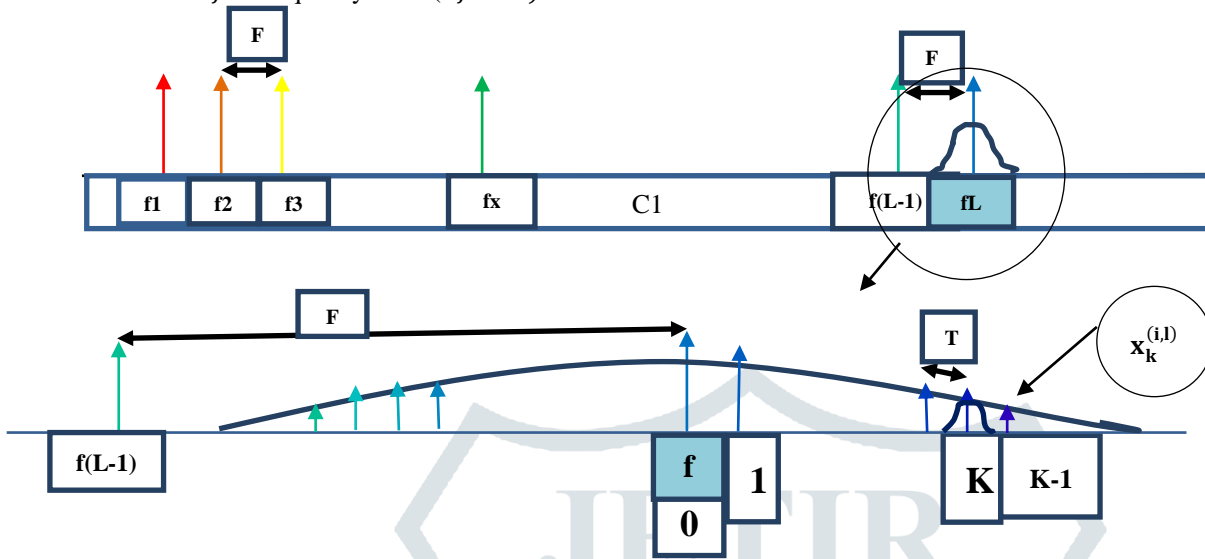


Figure: 8 X transmitted signal in frequency domain with $x_k^{(i,l)}$ symbol on l^{th} carrier and i^{th} polarization.[29]

They did first proper encoding with binary FEC and Gray code mapped onto QPSK constellation. This generated a stream of information bits. Then each and every transmitted symbols were taken from those stream of information bits. From mutual information $I(X;Y)$ property[47] we know;

Let, information rate or the average mutual information be $I(X;Y)_{avg}$. Entropy be $H(X)$, conditional entropy be $H(X|Y)$, where X be the transmitted signal(input symbol sequence) and Y be received signal(output symbol sequence).By mutual information property we can write:-

$$I(X;Y) = I(Y;X) .[47]$$

$$\text{or, } H(X) - H(X|Y) = H(Y) - H(Y|X).[47]$$

$$I(X;Y) = H(Y) - H(Y|X).[47]$$

$$\text{Or, } H(Y) - H(Y|X) = \sum_{l=0}^{K-1} P(Y_L) \cdot \log_2 \left(\frac{1}{P(Y_L)} \right) - \sum_{l=0}^{J-1} \sum_{l=0}^{K-1} P(Y_L) \cdot P(X_l|Y_L) \cdot \log_2 (1/P(Y_L|X_l)).$$

$$\text{Or, } H(Y) - H(Y|X) = \sum_{l=0}^{K-1} \sum_{l=0}^{J-1} P(Y_L) \cdot P(X_l|Y_L) [\log_2 \left(\frac{1}{P(Y_L)} \right) - \log_2 \left(\frac{1}{P(Y_L|X_l)} \right)].$$

$$\text{Or, } H(Y) - H(Y|X) = \sum_{l=0}^{K-1} \sum_{l=0}^{J-1} P(X_l) \cdot P(Y_L|X_l) [\log_2 \left(\frac{P(Y_L|X_l)}{P(Y_L)} \right)]. \quad (08)[47]$$

Where; $\sum_{l=0}^{J-1} P(X_l|Y_L) = 1$. The marginal probability distribution $P(Y_L) = \sum_{l=0}^{K-1} P(Y_L|X_l)P(X_l)$, [47] where; probabilities $P(X_l)$ for $l = 0, 1, 2, \dots, K-1$ are A Priori Probabilities (APP) of various input symbols.

From equation no.08 they wrote $I(X;Y)_{avg} = \lim_{K \rightarrow \infty} \frac{1}{2NcK} \cdot [I(X;Y)]$.

$$\text{Then Spectral Efficiency(SE)} = \frac{I(X;Y)_{avg}}{F \cdot T}. \quad (09)[29]$$

At Transmitter side:

According to their work, transmitted signal that was taken above were sent through dispersion uncompensated SMF(Single Mode Fiber). The fiber had many number of spans. A ROADM node was present on each and every two fiber spans. The span length was 120km SMF. Each span was followed by an EDFA(Erbium Doped Fiber Amplifier). A property of ROADM is such that it introduces a filtering effect of two WSS. It was like a super-Gaussian filter. Bandwidth of the filter was taken to be less than Flexi-grid channel spacing(37.5GHz). Signal propagation through fiber was impaired by GVD and non-linear effects. Split Step Fourier Method[48] were used for simulating those effects. Initially they took 32.5Gbaud symbol rate. For showing the benefits of Time Frequency Packing[49] technique they changed symbol rate to 75Gbaud and kept other parameters fixed. Even the filter bandwidth was kept fixed. They had to use 75Gbaud which was beyond Nyquist limit.

At Receiver side:

At receiver coherent detection was done by them. The optical signal was filtered using higher order super-Gaussian filter with 3dB bandwidth. Then it was converted to electrical signal by a 90° optical hybrid. After that, they did digital signal processing. Cumulated group velocity dispersion was reduced with the help of two fixed-tap Equalizers(two equalizers for two polarization). Then frame and frequency synchronization and reduction were done. An adaptive mean square error(MMSE) feed forward equalizer did the reduction of residual group velocity dispersion and polarization mode dispersion. It did polarization Demultiplexing too. Lastly, phase noise was traced with the help of a decision making phase estimation. Then phase noise was compensated(reduced) using compensation module. A MAP symbol detector and a channel reduction filter (linear filter) was also used.

They used only one carrier auxiliary channel to find the average IR(Information Rate) by assuming Group Velocity Dispersion and Polarization Mode Dispersion to be perfectly compensated and also avoided channel non-linearities. So they could not compute IR of actual channel that had multiple carriers.

Comparison and discussion

In general as the total span length of fiber increases spectral efficiency decreases and power required for launching increases. At starting distance(0 Km) spectral efficiency of MAP(Maximum-A-Posteriori) with length L=2 symbols is highest and MAP for L=1 symbol spectral efficiency is second highest and for symbol by symbol demodulation it's lowest. MAP demodulation has higher spectral efficiency and decreases at slower rate with respect to symbol by symbol demodulation. And launching power required for MAP,L=2 and L=1 symbols is lowest and it increases at slower rate as length of fiber span increases relative to symbol by symbol demodulation. They showed that for same baud rate MAP,L=1 symbol QPSK system has a increasing spectral efficiency as length of fiber span increases, while same baud rate 16-QAM symbol by symbol demodulation has a decreasing spectral efficiency as length of fiber span increases. Although increasing baud rate does make the spectral efficiency decreasing for MAP,L=1 symbol QPSK but the decreasing rate is slower with respect to 16-QAM symbol by symbol demodulation. However, if length of symbol L was increased to L=2 from 1, for MAP QPSK demodulation spectral efficiency got better. Advantage of using MAP demodulation over symbol by symbol demodulation is that it has better spectral efficiency and hence a signal can be sent at longer distance with least degradation.

In 2013 a work had been done by few authors, MengQiu, QunbiZhuge, Xian Xu, Mathieu Chagnon, Mohamed Morsy-Osman, and David V.Plant where they had proposed a less complex and more efficient carrier recovery algorithm in single carrier system. Frequency Offset in a signal is not a fixed incident, it varies[1],[2]. Their system was capable of tracing Frequency Offset(FO) variations. In optical communication systems coherent detection along with DSP had been used for quite a while now. There was an unintentional frequency offset introduced between Transmitter(Tx) Laser and Receiver(Rx) Local Oscillator Laser. Frequency fluctuation rate of an ECL was found to be around 0.2 MHz/μs in [2]. As this was small, accurate FO tracing was implemented on carrier recovery algorithm.

As they described, FO estimator algorithm for tracking FO between transmitter Laser and LO at receiver has two parts:-

- a) Estimation of Frequency Offset initially.
- b) Tracing of FO drift.

a) *Estimation of Frequency Offset initially*:- Firstly, estimation of the frequency mismatch of the received sequence in general was done. Training Symbol algorithm method[3] was used which gave an FO estimation range (-Rs/2 to +Rs/2, where Rs is symbol rate) before using Frequency Offset estimation algorithm.

b) *Tracing of FO drift*:- Secondly, using data sequence followed by training symbols, tracing of FO drift was done. Training symbols were identified from incoming received digitized symbols ($b_{Rx}(h)$) sequence as in figure below(Fig: (8)Block Diagram and Fig: (9)Symbol Sequence).

At the receiver end they had passed the received digital(binary) bit sequence $b_{Rx}(h)$ first through training symbols localization block where using Schmid algorithm the starting point of training symbol sequence was found.

Frequency Offset Estimation ($\Delta f_{est} \approx \Delta f_{o,k}$) was almost equal to Frequency Offset.



Figure: 9 Block Diagram of Training symbols and (FOE)Frequency Offset Estimation.[3]

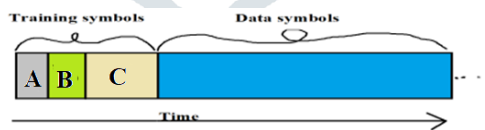


Figure: 10 Symbol Sequence.[3]

Then as initial FO estimation was done by them, tracing the FO drift was done by them using the data symbol sequence and then Training Symbols sequence[3] successively. At the moments of tracing, the data sequence was partitioned into blocks. Block length was L. That block was first pre-compensated with the help of estimated FO. There are $(k + 1)^{th}$ block which was later on processed for Carrier Phase Recovery. For getting FO estimation the following had been done by them, as shown in Figure 10 and equation(10) below.

$$\Delta f_{est} \approx \Delta f_{o,k} = (f_{o,(k+1)} - f_{o,k})/C \quad (10)[30]$$

Here, C was the previously obtained weight coefficient of the estimated FO variation. Depending on frequency drift the value of C is 1~2. Larger the value of C better was the performance when FO was drifting rapidly. The updated FO estimation $f_{o,k+1}$ was used for pre-compensating the next $(k + 2)^{th}$ block. This process of updating and pre-compensating was repeated as frequency offset variation was increasing as depicted in figure 11. This resulted in a good approximation of FO tracing after choosing the block length correctly and maintaining the FO drift inside a block to be very small (for instance, ~2MHz/ μs).

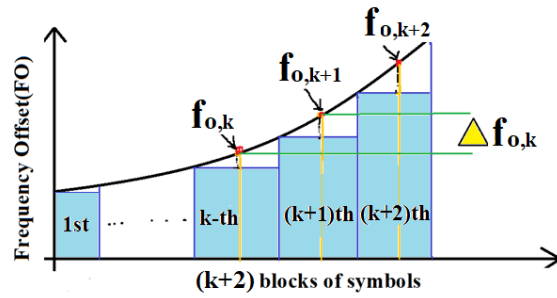


Figure: 11 FO Tracing Process.[30]

For estimating $\Delta f_{o,k}$, they further partitioned the block into sub-blocks. Every sub-blocks had Z symbols. They had calculated the increasing phase in the sub-block using Eqn.(11) below:

$$\Delta\varphi_i = \phi(z_i + Z) - \phi(z_i) \tag{11} [30]$$

Where, i was taken by them as the index of sub-block. The phase of the z_i^{th} symbol was $\phi(z_i)$. z_i is the index of the first symbol in i^{th} sub-block. Modulation had been removed with the help of a digital phase-locked loop. Other phase recovery algorithms like the Viterbi-and-Viterbi[1],[50] method could be used with this estimator. The phase increments was due to:-

- 1)Phase shift caused by unavoidable frequency offset [4].
- 2)Random phase errors came from unignored phase noise of a laser[4]. Laser phase noise came from additional neighboring spectral components of central frequency in a laser bandwidth.
- 3) Additive White Gaussian Noise(AWGN) [4].AWGN could be introduced in a channel.

However, it was observed that the average phase increment was mostly due to the phase shift caused by frequency offset. So, frequency offset $\Delta f_{o,k}$ was approximated by them using Eqn. (12):

$$\overline{\Delta\varphi} \approx 2\pi\Delta f_{o,k}ZT_{symbol} \tag{12}, [30] \text{ where, } \overline{\Delta\varphi} \text{ is Average Phase increment and } T_{symbol} \text{ is Symbol duration.}$$

According to them ,for high data rate systems, parallelization and pipelining were effective[5], [6]. After receiving the bit sequence they were de-multiplexed into parallel bit streams which were processed individually . It was being noted by them that the parallelization process not only enhanced impairments due to phase noise but also amplified the effects on the frequency offset and frequency offset drifts. More precisely, if the degree of parallelism is X as shown in Figure:12 *Parallelization*[4]. Frequency Offset was increasing by X times it's previous value in parallel de-multiplexed output from top to bottom. Hence, Phase shift between adjacent symbols due to Frequency Offset was consequently increasing by X times the previous original phase shift.

Therefore, according to them there was phase shift between adjacent symbols which was due to FO(Frequency Offset). The FO was augmented by X times in each successive de-multiplexed stream. And by same amount phase shift got augmented. If ECLs were used that had stable, narrow-linewidth laser sources in a system, the carriers of parallel bit streams did not differ that much among one another. When degree of parallelization was taken 'X' FO tracking estimator found FO($f_{o,k}$) for k^{th} block in that particular stream D(k,x).Then for FO compensation of next $(k + 1)^{th}$ block a factor ($F_{comp,k}$)was applied to that D(k,x) stream as well as next neighboring stream D(k+1,x). Thus, FO estimators on other streams were removed that also reduced overall complexity.

[The portion of this page is kept blank intentionally to make room for the figure.]

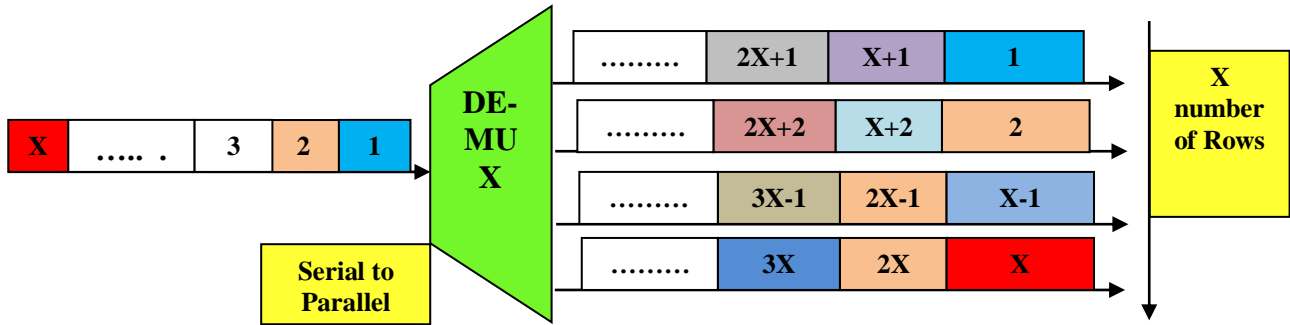


Figure: 12 Parallelization.[30].

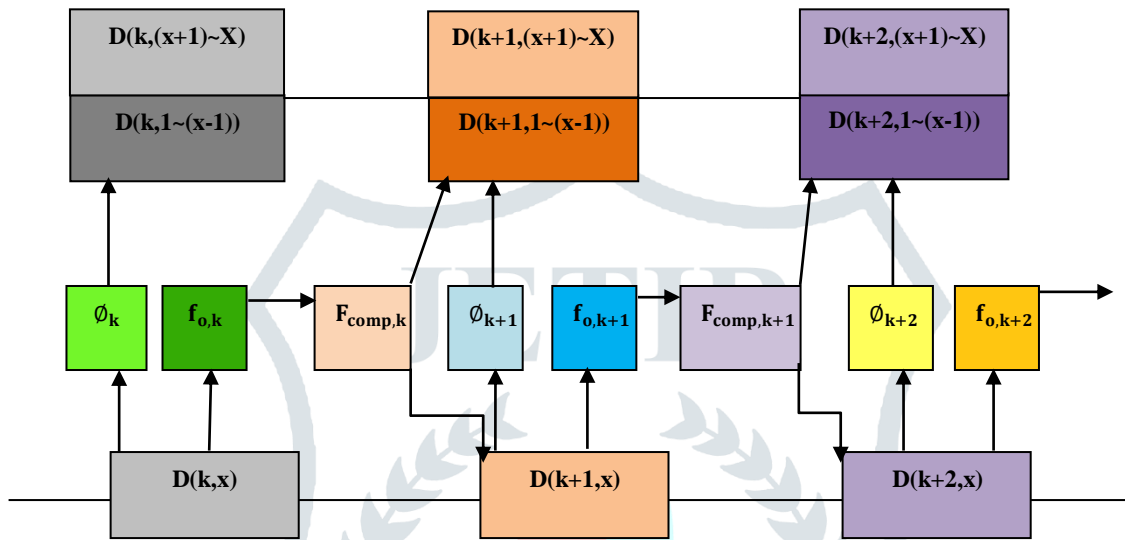


Figure: 13 Carrier recovery with parallelization.[30]

They were able to find out the frequency offset and also was able to trace the frequency offset drift. However there were some errors.

Comparison and discussion

Although FO drift estimation was able to trace FO drift but it had some estimation error(E). $E=|Actual\ FO\ drift - Estimated\ FO|$ drift which was very small and could be tolerated by CPR[51],[52],[1]. Without tracing, BER was found by them to be increasing at very higher rate than with tracing. When FO drift was in lower range (~ 0.1 to 0.2 MHz/ μs), in BER Vs OSNR plots, both for parallel streams and serial streams with tracing, BER curve was above theoretical BER curve and way below without tracing BER curve i.e; BER of parallel and serial streams is higher than theoretical BER and lower than without tracing BER as OSNR increases. When FO drift was in higher range (~2MHz/ μs or more), whole BER curve for parallel and serial streams and for theoretical BER moved up. The BER is now greater than before and now without tracing BER was so high that it couldn't be demodulated unless FO tracing was done. Disadvantage here is that, the FO was set around 1GHz which was very small with respect to larger FO=100GHz. In next section[31] we will see wider FO estimation which is above 1GHZ was done. A work in wider frequency offset estimation was done by Xian Zhou,XueChenandKeping Long in 2011-12 where they talked about the higher order PSK,QAM, formats which required future coherent optical transmission systems. In order to have higher spectral efficiency without compromising with the symbol rate or bandwidth increment higher modulation format was used. Due to large computational complexities and small estimation range in higher order modulation M^{th} power operation(for QPSK M=4) to remove the encoded phase information was not used before FOE . For 28Gbaud (or 28x4=112 Gbps) QPSK the estimation range was found to be $\pm R_s/8$, where R_s is symbol rate. Using Schmidh Algorithm it was required to find the beginning point of the training sequence in the whole digital received signal sequence and this training sequence would eventually give the range of the symbol rate($\pm R_s/8$).

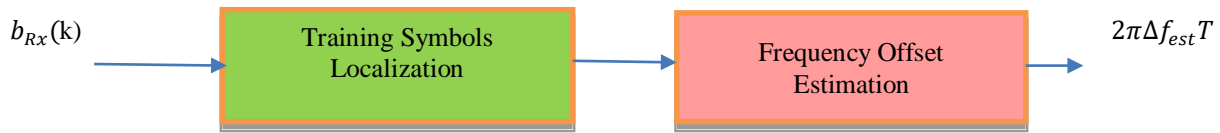


Figure: 14 Block Diagram of Training symbols and (FOE) Frequency Offset Estimation.[3]

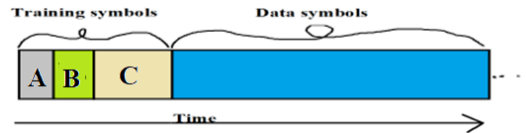


Figure: 15 Symbol Sequence.[3]

They explained, the digital signal $b(k)$ entering the FOE block would experience many impairments due to carrier phase error, the frequency offset and phase offset between transmitter Laser and receiver Local Oscillator. So, well correlation property must exist in the reception of training sequence. At the receiver a timing metric $M(t)$ was calculated as,

$$M(t) = \frac{|\sum_{m=0}^{L-1} [b^*(t+m)b(t+m+\frac{L}{2})]|^2}{\left(\sum_{m=0}^{L-1} |b(t+m)|^2\right)\left(\sum_{m=0}^{L-1} |b(t+m+L/2)|^2\right)}; M(t) \in [0,1] \quad (13).[31]$$

Where; t is the time index of the received symbol. $(\cdot)^*$ is a complex conjugate operation. $b(t)$ is received digital sequence and L is training sequence length in first stage.

Comparison and discussion

They generated a timing metric $M(t)$ Vs timing offset plot. It has a pyramidal curve whose peak(apex) is the beginning point of training sequence.

By finding maximum point of $M(t)$, the beginning point of the training sequence ($b_{ts}(k)$) could be identified after removing the modulated phase from $b_{ts}(k)$.

$$s(k) = b_{ts}(k) \cdot t_{ts}(k)^* \quad (14).[31]$$

Phase rotation due to frequency offset is;

$$2\pi\Delta f_{estimated}T = \arg \sum_N (s(k) \cdot s(k-1)^*) \quad (15).[31]$$

Where, T is symbol period. $\Delta f_{estimated}$ is estimated frequency offset. N is number of $b_{ts}(k)$. In theory estimation range of $\pm 1/2T$ was independent of signal modulation.

As it removed modulated phase from training sequence ($s(k) = b_{ts}(k) \cdot t_{ts}(k)^* = \sqrt{s(k)} \cdot e^{j\theta} \cdot \sqrt{s(k)} \cdot e^{-j\theta}$. Where, θ being some phase angle.) and it required no M^{th} power operation which reduced complexity compare to FOE in intradyne receiver[34] and also improved FOE from (0.125~0.625 GHz) to ± 13.9 GHz (approx.). Previously in FOE intradyne receiver[34] higher order PSK and QAM couldn't be used but now it could be in this paper where they found the FOE is $\sim \pm 13.9$ GHz. FO (Frequency Offset) tracking is $\sim \pm R_s/2$ GHz (where, R_s is symbol rate = 28Gbaud) which is far better with respect to previous Intradyne receiver FOE. Also in [31] Frequency Offset Estimation Error is $\sim \pm 10$ MHz for FO of $\sim \pm 13.9$ GHz which is very small compare to FOE in intradyne receiver[34]. In addition Wide range FOE using training sequence[31] has wider FOE range $\sim \pm 13.9$ GHz relative to QPSK partition method (using M^{th} power operation, where $M=4$ for QPSK)[53].

Another work had been done on wider and faster FOE by mentioned authors, Koichi Ishihara, Tadao Nakagawa, Riichi Kudo, Munehiro Matsui, Takayuki Kobayashi, Yasushi Takatori, and Masato Mizoguchi. In their paper they wrote, Carrier frequency offset must be estimated first. Then it should be compensated at the receiver (Rx). Many techniques and algorithms had been proposed earlier. In their paper the authors presented and simulated a blind frequency offset estimator. It had faster tracking time and wider frequency range. In blind receiver (Rx) m^{th} power algorithm had been widely used after finding the estimation range $\pm R_s/2m$, where R_s is symbol rate. m is number of constellation due to m^{th} power operation and phase variations. In 100Gbps (Polarization Multiplexed) PM-QPSK systems the estimation range was found to be $\pm \frac{R_s}{2m} = \pm 3.5$ GHz which was less than Frequency Offset (FO) of most commercial lasers ($FO \approx \pm 5$ GHz). Due to this mismatch in the FOE (Frequency Offset Estimation) of laser which was ± 5 GHz and m^{th} power estimation range ± 3.5 GHz there was a significant transmission quality degradation. The input PM-QPSK signal was passed through FFT block for getting frequency spectrum. Then the data in frequency domain was stored temporarily in a buffer memory. The output spectrum of buffer was passed through two rectangular windows. When the power difference $|P_p - P_M| > T_H$ was greater than a predetermined threshold T_H , the frequency components of input signal f_1, f_2, \dots, f_N were shifted cyclically. This cyclic shifting along frequency axis happened repeatedly until $|P_p - P_M|$ became smaller than T_H . The estimate FO could easily be deduced from total frequency shift distance (d) of spectrum.

The frequency shift/offset was given by:-

$$\Delta f = \Delta f_{estimate} = \frac{d \cdot n_{over} \cdot R_s}{N} \approx \Delta f_{offset} \quad (16).[32]$$

where, n_{over} is over sampling factor. R_s is symbol rate.

Time domain NCO (Numerically Controlled Oscillator) were not required.

Polarization Multiplexing QPSK with $R_s = 28$ GBaud = $28 \times 4 = 112$ Gbps modulation format was used.

The estimation accuracy was somewhat hampered by low pass filter cut off frequency(f_c) at receiver(Rx) because low f_c and large FO caused asymmetry of spectrum.

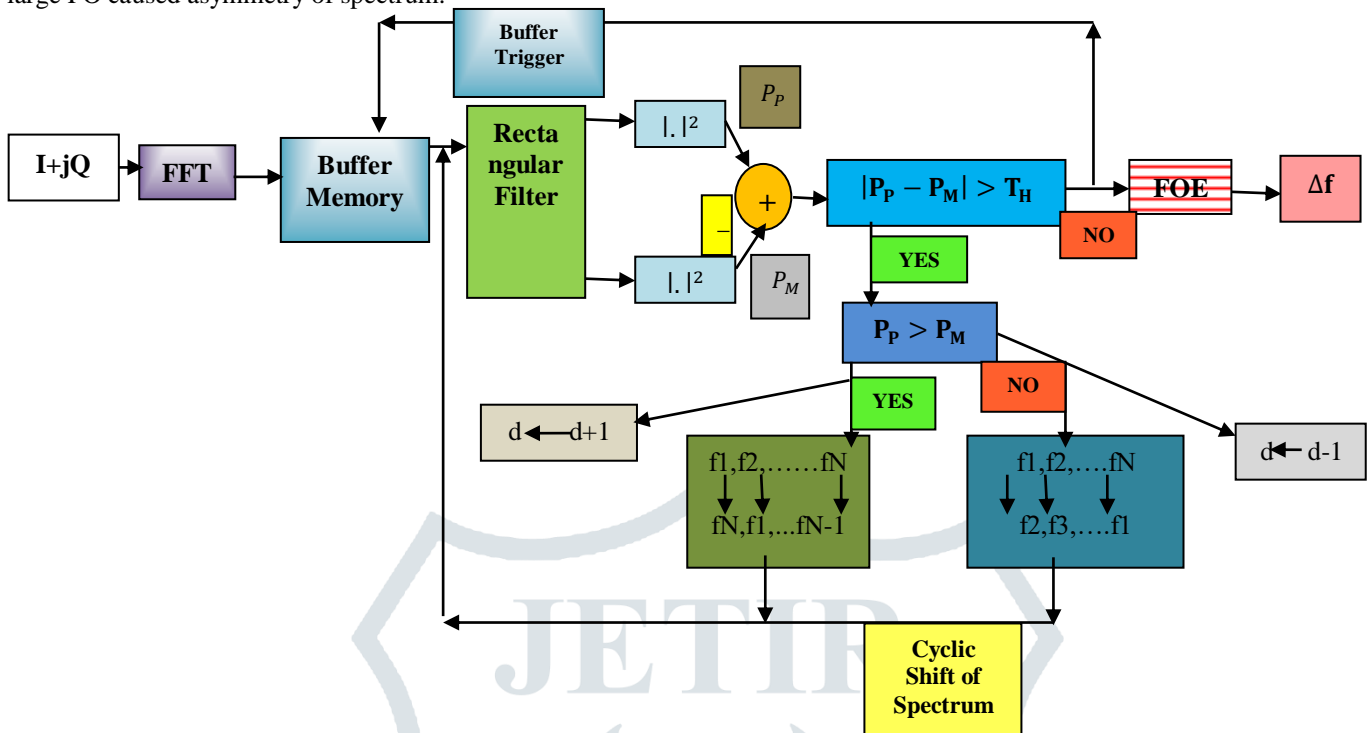


Figure: 16 (a) Block diagram of FOE.[32]

Comparison and discussion

In their generated FOE Vs actual FO plot, accuracy of FOE decreased(slope decreased) as cut off frequency of low pass filter decreased from 25GHz to 20GHz in QPSK systems. There FOE range was $\pm 5GHz$. Also in another plot they showed, for 4th power estimation method QPSK systems the accuracy of FOE decreases very less with respect to earlier one for lower low pass filter cut off frequency. However, FOE range reduced from $\pm 5GHz$ to $\pm 3.5GHz$.

In 2008 a work has been done by Pablo Gianni, Carmen E.Rodriguez,Graciela Corral-Briones,MarioR.Hueda and Hugo S.Carreron ultra-high speed intradyne coherent optical receivers.(for instance, $\geq 40Gbps$).

They combined a low latency DPLL to reduce FO(Frequency Offset) and frequency fluctuations due to mechanical vibrations. As we have seen, in feedforward CPR[51],[52], non-zero FO led to higher phase error variance. Laser frequency fluctuations can also be due to power supply noise. All these can deteriorate receiver(Rx) performance. Laser fluctuations was assumed to be similar to frequency modulation with larger amplitude and lower frequency($\leq 100KHz$) sinusoid. PADE(Pre-decision based Angle Differential frequency offset Estimation) method and other FO estimation algorithm[3] was inefficient to compensate that large frequency fluctuations and FO.So they introduced this new carrier recovery algorithm.This parallel DPLL approach takes out as much processing as possible from the feedback loop in order to simplify loop and reduce it's latency. They took QPSK modulation system.

According to them, n^{th} QPSK symbols(a_n) were transmitted through an EDC(Electronics Dispersion Compensation) the output of which was $r_n = a_n e^{-i\alpha_n + z_n}$ where, α_n was the total phase noise. z_n was the ASE noise that was modelled as white complex Gaussian random variable.

$$r_n = a_n e^{-i\alpha_n + z_n} \quad (17).[33]$$

$$\text{or, } r_n = s_n e^{i\theta_n} \quad (18).[33]$$

where, $s_n = |r_n|$ (magnitude of r_n) and $\theta_n = \angle r_n$ (angle of r_n) = $\zeta_n + \omega_c n + \Delta\omega_n + \phi_n$.

a) $\zeta_n \in \{\pm\pi/4, \pm 3\pi/4\}$.

b) ω_c (angular carrier frequency offset) = $2\pi f_c T$. f_c is carrier frequency offset, T is symbol duration.

c) $\Delta\omega_n$ is phase change due to frequency fluctuations.

$$\Delta\omega_n = \frac{A_p}{\Delta f_c} \sin(2\pi\Delta f_c Tn) \tag{19}.[33]$$

A_p and Δf_c are the amplitude and frequency of tone modulated signal. Here, carrier was modulated by sinusoid tone signal.

$$d) \phi_n = \phi_n^{(Laser)} + \phi_n^{(ASE)} \tag{20}.[33]$$

where, $\phi_n^{(Laser)}$ = phase noise from Laser. $\phi_n^{(ASE)}$ = Amplified Spontaneous Emission phase noise.

$$\phi_n^{(Laser)} = \sum_{k=-\infty}^n X_k = \sum_{k=-\infty}^n \frac{1}{\sqrt{2\pi(2\pi T\Delta\nu)}} e^{-\frac{1}{2}(\frac{k}{2\pi T\Delta\nu})^2} \tag{21}.[33]$$

Mean is zero, variance $\sigma^2 = 2\pi T\Delta\nu$. $\Delta\nu$ is laser linewidth.

A) System Model:-

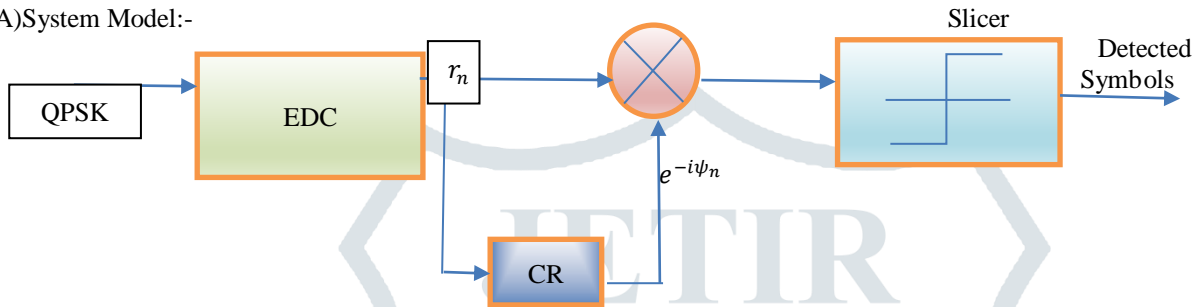


Figure: 16 (b) Coherent receiver with EDC.[33]

B) Carrier recovery and the reduction of frequency offset, frequency fluctuations:

A modified second order DPLL did the work of compensating frequency offset and frequency fluctuations. Their proposed block diagram is as follows:

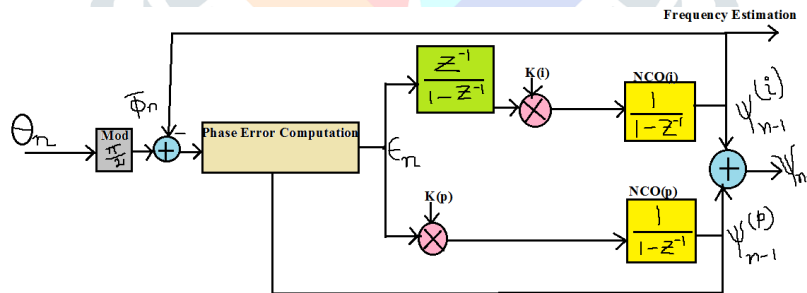


Figure: 17 Modified second order DPLL.[33]

The ϕ_n phase noise due to both Laser and ASE was passed through modulo M the output of which went into adder where frequency estimated signal was added and then the output went into phase error computational block. And the output came as phase error where one path out of two was passed through a delay and then multiplied with an integral gain ($K^{(i)}$) followed by a NCO (Numerically Controlled Oscillator) and the other path carries the same phase error which was multiplied with loop proportional gain ($K^{(p)}$) also followed by a NCO (Numerically Controlled Oscillator). Then these two outputs were added which gave the delayed phase (ψ_{n-1}) along with phase error ($K^{(p)}\epsilon_n$) and accumulated phase error ($K^{(i)}\bar{\epsilon}_{n-1}$).

$$\psi_n = \psi_{n-1} + K^{(p)}\epsilon_n + K^{(i)}\bar{\epsilon}_{n-1} \tag{22}.[33]$$

Comparison and discussion

In one of their generated OSNR penalty at 10^{-4} BER Vs tone amplitude (A_p) plot reveals:-

They explained, Mechanical vibration cause laser cavity size to be varying and that causes frequency fluctuation. This frequency fluctuation was taken by them as frequency modulation having large amplitude A_p also known as tone amplitude. ($A_p \sim 10\text{MHz}$ to 500MHz). Normally when they used serial and parallel Digital Phase Locked Loop for a specific filter length and other parameters kept constant OSNR penalty was increasing at higher rate as tone amplitude was increasing. Also same thing happened when only Viterbi-Viterbi CPR method was used. But, as soon as they used Viterbi-Viterbi method along with Serial DPLL, the OSNR

penalty reduced and became almost constant with increasing tone amplitude. Although in parallel DPLL processing speed was better but because of the presence of parallel structure that had P factor signal magnitude deterioration was slightly larger than serial DPLL. And also OSNR penalty was slightly higher with respect to serial DPLL.

In 2007 a work had been done on frequency estimation by fellow authors, Noriaki, Kaneda, Andreas Leven, Ut-Va-Koc, Young-Kai-Chan where for larger frequency gap between transmitter laser and local oscillator laser at optical intradyne receiver, first the frequency estimation was done. Then phase estimation and other phase recovery procedures were done. Phase shift existed between two adjacent samples a_k, a_{k+1} which was due to frequency offset Δf between transmitter Laser and LO Laser. The purpose of frequency estimator was to approximately find out amount of phase shift $\Delta\phi$.

Phase Locked Loop(PLL) was used to take care of the phase and frequency differences respectively between tunable ECL(External Cavity Laser) at transmitter and LO Receiver. This frequency differences could be seen as the rotation of QPSK constellation in complex (I-Q) plane. So digital frequency estimation were used to replace PLL and FLL in intradyne receiver.

Received signal/symbol a_k was multiplied with complex conjugate of previous(past) symbol and the result had a phase which was equal to phase difference between two successive symbols(a_k, a_{k+1}^*). Any information encoded in signal phase had to be removed. In PSK signals, n^{th} power of complex symbol. Here, n is number of constellation points. In QPSK $n=4$, so the result was taken by them as power of four and summed up(performed average operation) over a large number of samples(~500 samples). Argument $\arg(\cdot)$ which was the phase had to be divided by $n=4$ for QPSK to correct the previous power of four $(\cdot)^4$ operation. Result they got was the phase offset $\Delta\phi$. Here, $\Delta f = \Delta f_{estimate} = \text{Frequency Offset}$.

$$\Delta\phi = 2\pi\Delta f T_s \tag{23}, \text{Where, } T_s \text{ is sampling time. [34]}$$

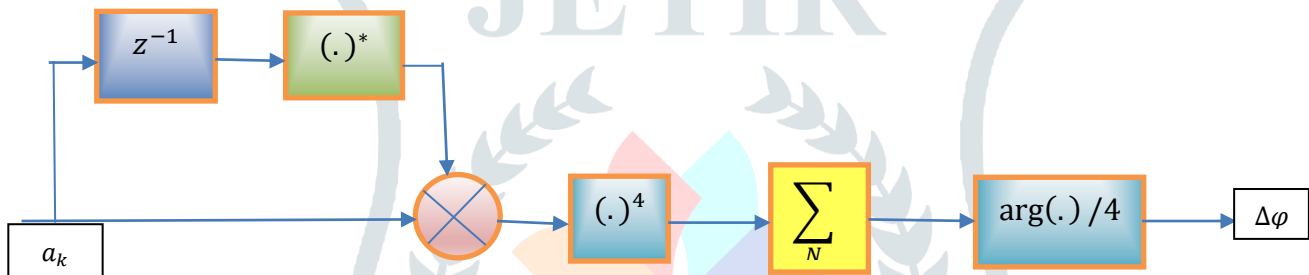


Figure: 18 Frequency estimator Block diagram.[34]

For correcting frequency offset, the accumulated phase offset

$$\phi = 2\pi\Delta f T_s \tag{24 a).[34]}$$

was subtracted from each symbol a_k where 'k' being a symbol index. It was subtracted to get corrected symbol. And this symbol was processed using phase estimation methods.

Comparison and discussion

As the frequency offset(FO), Δf was nominally changed from 0 to 1.5GHz in steps of 0.25GHz in differential decoding detection the Δf of 0.5GHz(or ~500MHz) had 7dB OSNR penalty but the proposed Block Phase Estimation(BPE) had no penalty which is better. Also the BER(Bit Error Rate) of the BPE was reduced for higher OSNR with respect to BER of differential decoding detection. Without Frequency Estimator maximum allowable frequency offset for Block Phase Estimation was 125MHz. Frequency Offset for differential decoding detection was 625MHz. Maximum allowable FO was given by them as;

$$\Delta f_{max} = 1/(2.l.n.T_s) \tag{24 b).[34]}$$

where, l is length of samples=2 for differential detection. $n=n^{th}$ power operation(n slices in complex plane). T_s is symbol rate. **Homodyne Receiver(Rx):**-The receiver where Transmitter(Tx) Laser frequency is ideally same as the frequency of received RF signal and LO(Local Oscillator) Laser.

In RF(Radio Frequency) Homodyne receiver no mixer and LO is required. Modulated received RF signal is directly applied to I/Q Demodulator before demodulation.

If RF frequency signals and LO frequency signals are equal then no LO and mixer is required, i.e; $(f_{IF}=f_{RF}-f_{LO} = 0)$ where, f_{IF} is Image Frequency, f_{RF} is received Radio Frequency and f_{LO} is Local Oscillator(LO) frequency.

Heterodyne Receiver(Rx):-The receiver where the demodulation is done such that Transmitter(Tx) Laser frequency is not same as LO(Local Oscillator) Laser. And Transmitter Laser frequency may differ from LO Receiver frequency by more than signal(message) bandwidth.

Also, in RF Heterodyne receiver when the received Radio Frequency(f_{RF}) does not match the I/Q Demodulator input Image Frequency(f_{IF}), received RF signal is mixed or heterodyned with Local Oscillator(LO) signal for either up conversion or down conversion of the received RF(f_{RF}). The receiver where the heterodyning or mixing is done twice in a row(cascaded) for larger frequency gap between f_{IF} and f_{RF} it is called Super Heterodyne Receiver.

Intradyn Receiver(Rx):-The receiver which is a combination of both Homodyne and Heterodyne receiver where the demodulation is done such that Transmitter(Tx) Laser frequency differs very little from LO(Local Oscillator) Laser. Transmitter Laser frequency differs from LO Receiver frequency by less than signal(message) bandwidth. Here it has minimum receiver processing bandwidth and requires no optical phase synchronization.

Why intradyne receiver Laser was used? It was used because of low power consumption, higher data rate along with reduced hardware complexity for higher order modulation formats.

In 2007 a work on feed forward carrier recovery was done by Joseph M.Kahn and Ezra Ip fellow members of IEEE where they used feed-forward mechanism instead of any electrical Digital Phase Locked Loop(DPLL) because the slightest of the propagation delay was causing the phase loop instability. In addition, PLL was less tolerant to Laser phase noise and it also had frequency mismatch between the transmitter laser and local oscillator laser . So they had introduced a MAP(Maximum-A-Posteriori) concept. This concept made things easier for detecting both transmitter symbols and carrier phase jointly. Due to mismatch in phases between LO Receiver(Rx) and Transmitter(Tx) Laser there was a phase offset and hence phase noise was also there which was a major impairment in coherent optical communication. Previously, Electrical or Optical Phase Locked Loop(PLL) were used to take care of the phase offset and frequency offset between transmitter laser and local oscillator receiver laser. But PLLs were sensitive to propagation delay inside the loop. It had been found that for 10 Gbps transmission, when delays became larger than some nano seconds time, it caused loop instability. Although by vigilant and precautionary design propagation delay could have been reduced but coherent demodulation where PLL was present had strict(inflexible) linewidth demands. Tunable ECL(External Cavity Laser) had linewidths in order of 10 to 100 KHz so 8-QAM was barely feasible and 16-QAM was not feasible at all. VLSI technology i.e; Analog to Digital Converter helped in converting in phase(I) and quadrature phase(Q) components of analog signal in homodyne optical receiver into digital output. Unintentional FO(Frequency Offset) and PO(Phase Offset) was reflected in the rotation of QPSK constellation. These had been tracked using DSP(Digital Signal Processing) and had been reduced in feedforward architecture.

Receiver Model:-

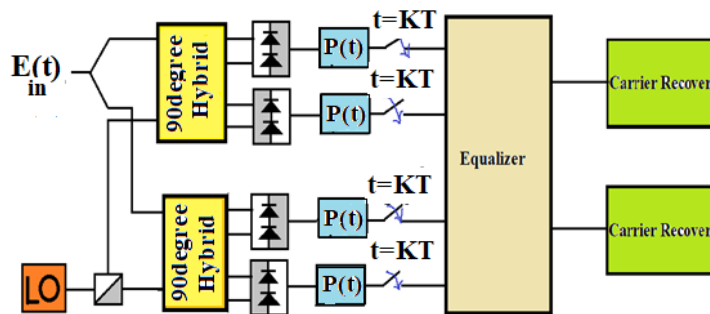


Figure: 19 polarization diversity homodyne receiver.[35]

They had used a polarization diversity homodyne receiver. Polarization beam splitter divided the local oscillator light into two different polarized lights(like for instance, horizontal and vertical polarized lights). These two different polarized lights were mixed separately with the received optical signal $E_{in}(t)$ in two separate 90° Hybrids. Then it generated four vertically polarized lights $P_{1aV}(t), P_{1bV}(t)$ and $P_{2aV}(t), P_{2bV}(t)$ in upper ninety degree hybrid as in figure 21,[36]. And four horizontally polarized lights $P_{1aH}(t), P_{1bH}(t)$ and $P_{2aH}(t), P_{2bH}(t)$ in lower ninety degree hybrid. These upper four vertically polarized light components were passed through two upper balanced photo detectors for converting optical components to electrical in phase(I) and quadrature phase(Q) vertical components. And lower four horizontally polarized light components were passed through two lower balanced photo detectors for converting optical components to electrical in phase(I) and quadrature phase(Q) horizontal components. These four electrical signal components were passed through low pass filter. Then these were sampled above Nyquist rate at every $t=KT$ switching and finally converted to digital signal with the help of high speed Analog-to Digital Converter(ADC). This above mentioned technique and low power penalty linear equalizer reduced chromatic dispersion. It also reduced polarization mode dispersion. They also assumed equalizer had no ISI(Inter Symbol Interference) and Non-Linearities. In addition carrier recovery was done for each channel separately. Input to carrier recovery had form:-

$$y_k = x_k e^{i\theta_k + n_k} \tag{25}.[35]$$

Let, $x_k e^{i\theta_k} = A$,

Where, θ_k is the carrier phase. n_k is the AWGN (Additive White Gaussian Noise). x_k is complex transmitted symbol.

MAP symbol by symbol detection:

$$P(y_k | x_k, \theta_k) = \frac{1}{\pi N_o} \times e^{-\left\{ \frac{|y_k - x_k e^{i\theta_k}|^2}{N_o} \right\}} \tag{26}.[35]$$

Joint MAP estimation of the sent symbol and carrier phase are:

$$(\hat{x}_k, \hat{\theta}_k) = \max_{x_k, \theta_k} P(y_k | x_k, \theta_k) P(x_k) P(\theta_k) \tag{27}.[35]$$

According to them for Data Assisted Phase Estimation (DAPE), training symbols were sent. So, MAP estimate could be written simply as;

$$\hat{\theta}_k = \max_{\theta_k} P(y_k | x_k, \theta_k) = \arg\{y_k\} - \arg\{x_k\} \tag{19}$$

$$\max_{\theta_k} P(y_k | x_k, \theta_k) \approx \max_{x_k} [\max_{\theta_k} P(y_k | x_k, \theta_k)]. \tag{28}.[35]$$

Where, $P(y_k | \theta_k) = \sum_{m=0}^{M-1} P(y_k | x_k = x_m, \theta_k) P(x_k = x_m)$ (29).[35]

MAP sequence detection:

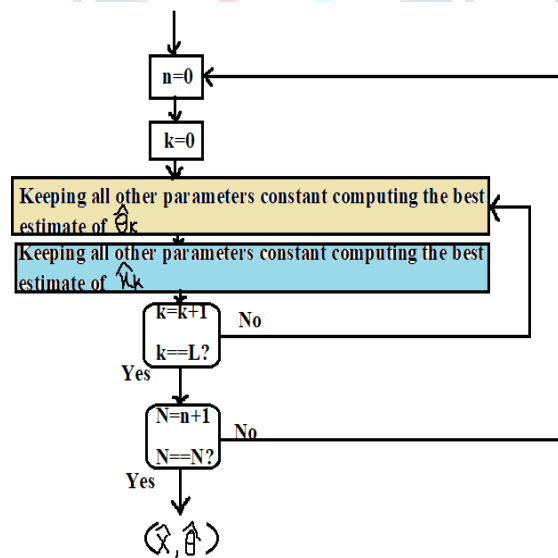


Figure:20 Algorithm for estimating x and θ . [35]

Comparison and discussion

In the receiver they used a soft and a hard decision phase estimation stages. This was for estimating carrier phase and phase of imparted symbol. Soft decision phase estimator was used in two cases which had been mentioned. One was NDA phase estimator (suitable for M-PSK transmission) and the other was DD phase estimator (suitable for any general constellation). [54].

In their plot of phase error standard deviation (S) Vs filter delay (d), soft decision Wiener filter had higher and increasing value of S. And hard decision Wiener filter had lower and almost constant value of S for increasing delay (d). So, soft decision was a big disadvantage as there were cycle slips that hampered PLL. It also hampered feed forward carrier recovery.

Also, in their plot of standard deviation (S) Vs filter delay (d) for a specific filter length (l), S for Wiener filter is least and almost constant. S decreases at smaller delay and then increases for larger delay in uniform filter. So, Wiener filter had the best performance for any delays. Uniform filter had the poorest performance.

One shot estimator used by them was not affected by any delay at all. This was because only one shot phase was taken into account for a particular symbol period.

Again, in their plot of bit error probability(P) Vs delay(d), in general every modulation format system had a maximum and a minimum bit error probability that changes with changing delay. Maximum P value increasing rate is faster than minimum P value. To their surprise they found lowest order QAM had less and slow increasing bit error probability as bit linewidth was increasing. Which means, 4 QAM had the least increasing rate of bit error probability, 8 QAM was intermediate and 16 QAM had the fastest increasing rate of bit error probability for increasing bit linewidth.

In 2008-2009 a work on phase estimation had been done by Michael G. Taylor. In that paper several phase estimation methods were mathematically modeled. Like, MAP(Maximum-A-Posteriori) phase estimation, decision directed phase estimation, power law average phase estimation(using Weiner Filter),Power Law PLL phase estimation. Previously, coherent detection was mainly studied for optical gain. Nowadays several optical amplifier is taking care of optical gain so the interest on coherent detection study had been shifted from optical gain to the features of coherent detection. A coherent receiver responded to a light in neighboring spectrum of local oscillator laser which was equivalent to Ultra narrow WDM optical filter in front of receiver(Rx) and which was also equivalent to tunable wavelength LO Laser. Chromatic Dispersion could effectively be compensated by DSP(Electrical) of intermediate frequency signal. Coherent demodulation was sensitive to phase of optical signal. So PSK signals (like, BPSK,QPSK,MPSK) and QAM signal formats were chosen as they are more sensitive to optical signal phase relative to sensitivity of amplitude modulated formats(ASK/OOK).

They described the followings:-

- i)How MAP phase estimation was calculated.
- ii)The Decision Directed phase estimation.
- iii)Power law average phase estimation and it's Weiner filter Transfer Function(TF).
- iv)Look ahead computation of the signal used for parallel digital signal processor.
- v)Q factor penalty against linewidth of different phase estimation.
- vi)Effect of cycle slip on received data signal. Reduction of negative impact of cycle slip with the help of differential logical detection.

As they explained well in their paper, the figure below depicts the set up of a coherent digital receiver. Optical signal $E_s(t)$ was heterodyned with local oscillator light E_{LO} in 90° Hybrid which was made up of waveguide coherent detection with DSP[10],[11],[12] or Polarization Beam Splitter[13],[10] or passive Coupler[14]. The lowermost arm of the LO Laser was quarter cycle longer than the upper arm of LO Laser and due to which the lowermost arm offered 90° phase shift. So the Balanced Photo Detector could see the upper arm of LO Laser light and the optical signal were in phase(I). While the Balanced Photo Detector could see the lower arms of LO Laser light and lower arm of optical signal were in quadrature phase(Q). The two powers P_{1a} and P_{1b} of the upper arm were mathematically expressed by them as:-

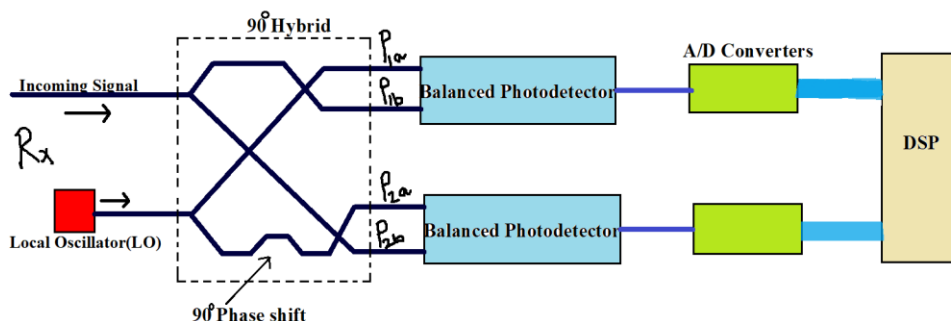


Figure: Coherent Detection using DSP

Figure: 21 Coherent detection using DSP.[36]

Local oscillator laser SOP(State Of Polarization) was constant. And signal's SOP might change over time. Which means the electric field envelope of signal changes. But the electric field envelope could be found using Jones Vector. Jones Vector can be expressed as:-

Let light ray with instantaneous E vector be,

$$\vec{E}(z, t) = \hat{i}E_x(z, t) + \hat{j}E_y(z, t). \quad (30)$$

Where, $E_x(z, t) = E_{ox}e^{i(kz - \omega t + \phi_x)}$, $E_y(z, t) = E_{oy}e^{i(kz - \omega t + \phi_y)}$. E_{ox} and E_{oy} are relative amplitudes and ϕ_x and ϕ_y are relative phases.

$$\text{Or, } \vec{E}(z, t) = \vec{E}_0 \cdot e^{i(kz - \omega t)}. \text{ Where, } \vec{E}_0 = \hat{i}E_{ox}e^{i(\phi_x)} + \hat{j}E_{oy}e^{i(\phi_y)}.$$

$$\text{Or, } \vec{E}_0 = \begin{bmatrix} \vec{E}_{0x} \\ \vec{E}_{0y} \end{bmatrix} = \begin{bmatrix} E_{ox}e^{i(\phi_x)} \\ E_{oy}e^{i(\phi_y)} \end{bmatrix} = e^{i(\phi_x)} \cdot \begin{bmatrix} E_{ox} \\ E_{oy}e^{i(\delta)} \end{bmatrix}. \text{ Where, } \delta = \phi_x - \phi_y.$$

Similarly, from the equation(22) ;

$$E_s(t) = \frac{[\exp(-i(\omega_s - \omega_{LO})t - i\phi_s(t) + i\phi_{LO}(t))] \times (\Delta P_1(t) + i\Delta P_2(t))}{4E_{LO}^*}. \quad (31).[36]$$

We know, Jones Vector;

$$\vec{E}_s(t) = \begin{bmatrix} \vec{E}_{s1} \\ \vec{E}_{s2} \end{bmatrix} = \begin{bmatrix} 4\text{Re}[E_s(t)E_{LO}^* e^{i(\omega_s - \omega_{LO})t + i\phi_s(t) - i\phi_{LO}(t)}] \\ 4\text{Im}[E_s(t)E_{LO}^* e^{i(\omega_s - \omega_{LO})t + i\phi_s(t) - i\phi_{LO}(t)}] \end{bmatrix}.$$

$$P_{1a}(t) = |E_s(t)|^2 + |E_{LO}|^2 + 2\text{Re}[E_s(t)E_{LO}^* \exp(i(\omega_s - \omega_{LO})t + i\phi_s(t) - i\phi_{LO}(t))]. \quad (32).[36]$$

$$P_{1b}(t) = |E_s(t)|^2 + |E_{LO}|^2 - 2\text{Re}[E_s(t)E_{LO}^* \exp(i(\omega_s - \omega_{LO})t + i\phi_s(t) - i\phi_{LO}(t))]. \quad (33).[36]$$

The output of the balanced photodetector was:-

$$\Delta P_1(t) = P_{1a}(t) - P_{1b}(t)$$

$$\text{Or, } \Delta P_1(t) = 4\text{Re}[E_s(t)E_{LO}^* \exp(i(\omega_s - \omega_{LO})t + i\phi_s(t) - i\phi_{LO}(t))]. \quad (34).[36]$$

Where, t is time.

ω_s is angular frequency of optical signal (in $\frac{\text{radian}}{\text{second}}$). $E_s(t)$ is complex envelope of the electric field of optical signal.

E_{LO} is complex envelope of LO electric field.

$\phi_{LO}(t)$ is phase of Local Oscillator(LO).

ω_{LO} is angular frequency of Local oscillator(LO).

$$\Delta P_2(t) = 4\text{Re}[-iE_s(t)E_{LO}^* \exp(i(\omega_s - \omega_{LO})t + i\phi_s(t) - i\phi_{LO}(t))]. \quad [36]$$

$$\text{Or, } \Delta P_2(t) = 4\text{Im}[E_s(t)E_{LO}^* \exp(i(\omega_s - \omega_{LO})t + i\phi_s(t) - i\phi_{LO}(t))]. \quad [36]$$

$$E_s(t) = \frac{[\exp(-i(\omega_s - \omega_{LO})t - i\phi_s(t) + i\phi_{LO}(t))] \times (\Delta P_1(t) + i\Delta P_2(t))}{4E_{LO}^*} \quad (35).[36]$$

After sampling at sampling rate (also symbol period) nT_s

Where, $n = 1, 2, 3, \dots$ etc.

Here they took $T_s = 1$ second for convenience.

Estimating phase using MAP :

Although MAP estimation could be calculated theoretically but it was impractical to estimate in a real time DSP. They had mentioned, for practical estimation scenario power law average estimate using Weiner filter was the best.

Laser phase noise along with the increase of number of bit errors could cause cycle slips which could be dealt with by using differential logical detection.

$E_s(t)$ was converted from continuous time(t) domain to discrete time(n) domain $E_s(n)$.

$$E_s(n) = b(n)E_{s0}\exp(i\omega_s t + i\phi_s(n)) + P(n)E_{s0}\exp(i\omega_{LO} t + i\phi_{LO}(n)). \quad (36).[36]$$

Where, $b(n)$ is digital information encoded on signal i.e; here M-ary PSK modulation formats ($M=2,4$ binary and quadrature respectively) used.

For $M=2$ i.e; BPSK $b(n) = \{-1, 1\}$. [56]

$M=4$ i.e; QPSK $b(n) = \{-1-j, -1+j, +1-j, +1+j\}$. [56]

$P(n)$ is a complex Gaussian Noise sequence with variance σ_p^2 .

At coherent receiver the phase was:-

$$r(n) = \frac{\Delta P_1(n) + i\Delta P_2(n)}{4E_{LO}^* E_{s0}}. \quad (37).[36]$$

$$\text{or, } r(n) = b(n)\exp(i\omega t + i\phi(n)) + p(n) \quad (38).[36]$$

where,

$\omega = \omega_s - \omega_{LO}$ also, it's a frequency offset.

$\phi(n) = \phi_s(n) - \phi_{LO}(n)$ also, it's a phase offset.

So, when the local oscillator laser light and the signal light had Lorentzian shape then the phase noise ϕ was Gaussian random function. See Weiner process [55].

$$\phi(n) = \phi(n-1) - w(n) \quad (39).[36]$$

Given, $w(n)$ as a (real) Gaussian noise sequence of variance, and

$$\sigma_w^2 = 2\pi T_s \Delta\nu. \quad (40).[36]$$

Where, $\Delta\nu$ is the combined linewidth (total of Full Width Half Maximum (FWHM) linewidths of the signal and Local Oscillator (LO) lasers).

The MAP estimation was the best possible estimate of the phase that could be done given the observed values $r(n)$. In addition it (MAP estimation) had the sequence of values that maximized the log-probability function,

$$\text{Log}_e(P) = \sum_n \left(-\frac{|r(n) - \hat{b}(n)\exp(i\hat{\phi}(n))|^2}{2\sigma_p^2} - \frac{(\hat{\phi}(n) - \hat{\phi}(n-1))^2}{2\sigma_w^2} \right) \quad (41).[36]$$

provided that statistical property of the phase noise and additive noise is known.

Comparison and discussion

Although MAP was the best estimation method of all, the disadvantage of MAP was that, it could not be done by real digital processor but could be done only mathematically.

In 2012 a work had been done by few authors, Qunbi Zhuge, Mohamed Morsy-Osman, Xian Xu, Mohammad E. Mousa-Pasandi, Mathieu Chagnon, Ziad A. El-Sahn, and David V. Plant on a Modified Super Scalar Parallelization technique used in Phase Locked Loop (M-SSP-PLL) along with Maximum-Likelihood (ML) phase estimator was used. This helped in Carrier Phase Recovery (CPR). In Comparison to the original SSP-PLL, the new technique used by them decreased the size of buffer needed with the help of a unique superscalar structure. Also, the performance of CPR (Carrier Phase Recovery) got improved there, after discarding the earlier differential coding-decoding and by introducing ML phase estimator. Carrier Phase Recovery (CPR) was a very important Digital Signal Processing (DSP) procedure in coherent receiver systems. CPR was done to reduce the random phase

changes caused by the transmitter laser and the local oscillator laser [16– 18]. According to them CPR algorithm should have three properties:-

- 1) Low computational complexity.
- 2) High tolerance for laser linewidth.
- 3) Applicability should independent on the type of modulation format.

According to them, the first and third requirements could be fulfilled by a general digital phase locked loop (DPLL). But a greater feedback delay was introduced because of the parallelized and pipelined technique used in fast performing optical receivers. Thus, laser linewidth tolerance became inefficient [16, 17]. *Viterbi and Viterbi* [1],[50] algorithm was very good for QPSK systems because computation was simpler and tolerance for laser linewidth was better[16, 18]. But without modifying the QPSK systems, like QPSK partitioning for 16-QAM [19, 20],it could not be used for higher QAM formats. Although the algorithm was more complex, Blind Phase Search (BPS) mentioned in [17] was considered to be the best tolerance for laser linewidth in any QAM formats.

In their work, they had described in depth the Modified Super Scalar Parallelization technique used in PLL (M-SSP-PLL)in tandem with their proposed earlier work [21], Linewidth-tolerant low complexity pilot-aided carrier phase recovery for M-QAM using superscalar parallelization.

Three modifications those had been made by them in their algorithm are:-

- 1) For each parallelization in QPSK about 200 buffer symbols were used. One percent pilot overhead symbol in 16, 64 -QAM, about 400 buffer symbols were used. In[22] more than 1024 buffer symbols had been utilized.
- 2) Differential coding-decoding in SSP-PLL was futile so it had been removed. Removing it did enhanced the performance somewhat.
- 3)Performance was still hindered because of feedback delay($P \times D$) in pipelined processing. For enhancing even more performance they made use of Maximum Likelihood algorithm after SSP-PLL.

Super Scalar Parallelization based carrier phase recovery:

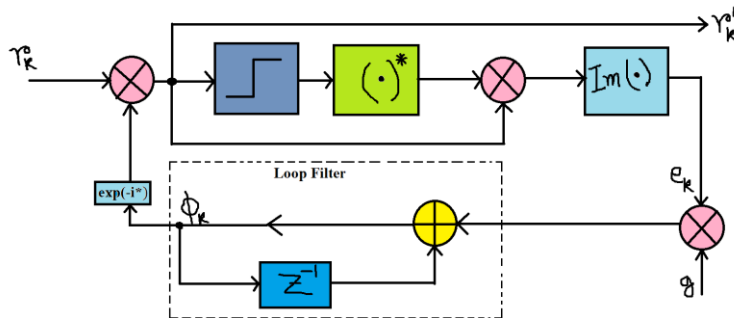


Fig: Block diagram of first order PLL

Figure: 22 First order PLL.[37]

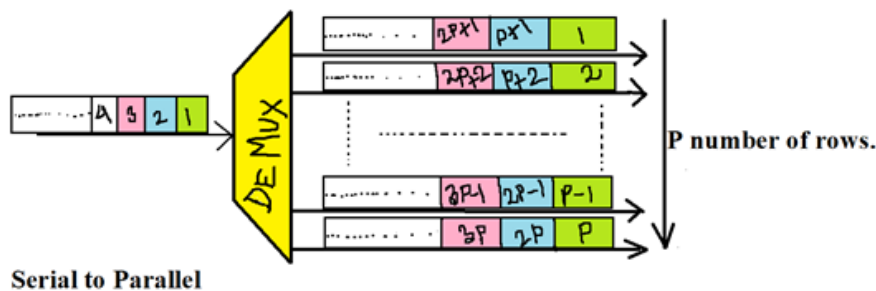


Figure: 23 Parallelization.[37]

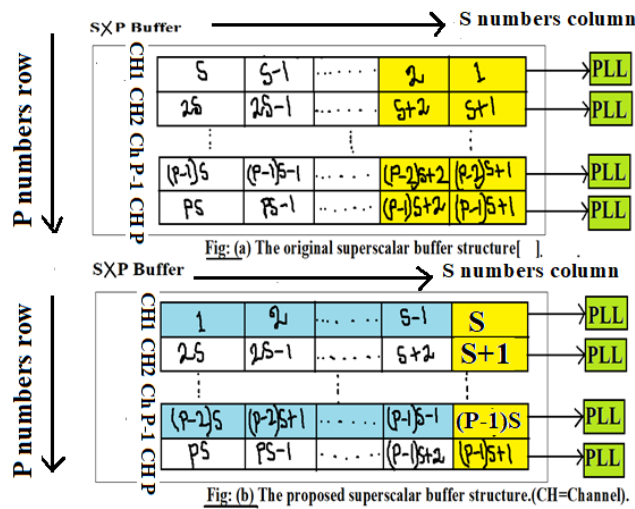


Figure: 24(a)Older superscalar buffer structure. (b)New updated superscalar buffer structure.[37]

For removing propagation delay P due to interleaving parallelization and thereby improving performance, Super Scalar Parallelization Phase Locked Loop(SSP-PLL) was proposed in[17]. There it was described how it used an $S \times P$ symbols sized buffer to store the input symbols. Given, S as each block length. As depicted in Fig:(a) stored symbols were rearranged so that they(symbols) are consecutive in each parallel channel. Although, two large sized buffers were required one for arranging symbols in consecutive order in each parallel channels and other buffer for arranging back to previous original sequence after processing had been done. Then, PLL feedback delay $P \times D$ decreased to D symbols. Furthermore, PLL processing had no relationship among the blocks in each channel. So a pilot symbol as highlighted with yellow color in Fig:(a) were needed at the starting end of each block. That resulted in a pilot symbol overhead.

Also they had mentioned Modified SSP-PLL(M-SSP-PLL) in [21]. This had reduced the buffer size and had improved the tolerance of linewidth of laser. They had noticed that the performance of SSP-PLL was hindered less due to block length S and more due to overhead of pilot symbol. the buffer size S was inversely proportional to overhead of pilot symbol.

$$\text{i.e; Overhead} = \frac{N_{PS}}{S} \tag{42}.[37]$$

Given, N_{PS} is pilot symbol numbers in each block.

So to decrease the buffer size S without making the overhead of pilot symbol larger, they had mentioned a unique superscalar structure. This structure is given in Figure: (24)(b) above.

Comparison and discussion

In their generated OSNR penalty(O) Vs symbol duration multiplied linewidth plot(symbol linewidth), for QPSK, 16, 64 QAM systems OSNR penalty was least for M-SSP-PLL+ML[37]. Also, penalty was increasing at slower rate than O-SSP-PLL, ILP-PLL+ML[37] and faster rate than BPS. OSNR penalty of BPS was not least however, increasing rate was slowest. Performance deterioration of BPS was least of all. So BPS wins here by virtue of it's slowest increment of OSNR penalty rate with increasing symbol linewidth.

In other plots of BER Vs block length and Pilot symbol QPSK had the lowest and near constant BER. 16 QAM had second lowest BER and 64 QAM had highest BER.

In their BER Vs OSNR plot, M-SSP-PLL+ML had least BER and fastest decreasing rate with increasing OSNR. So it was the best of all. BPS ranked second in this category.

Also, in their BER Vs distance plot, M-SSP-PLL+ML had slowest increasing rate BER for increasing distance. So it was the best of all. Again, BPS ranked second in this category.

In addition, M-SSP-PLL+ML was found to have 0.5 dB OSNR more than BPS. And one fourth transmission distance increment over BPS. Performance was better than BPS. And it was less complex. Ultimately, M-SSP-PLL+ML was the winner of all.

In 2014 a work was done by few respected authors QunbiZhuge, Mohamed Morsy-Osman, Mathieu Chagnon, Xian Xu, MengQiu, and David V. Plantwhere they had proposed a less complex, usable for any modulation formats, with flexible bandwidth and less energy consuming DSP based transceiver. Where they used QPSK symbols as both the training symbols for the frequency offset tracking and also the pilot symbols for initialization at the receiver-side DSP for various modulation formats QPSK, 8QAM,16QAM and 64QAM. Previously turning on and off the laser the sub-channel's bandwidth were allocated. Then later on, channel bandwidth allocation had been done in digital domain. This had drastically improved the performance of higher order QAM. For making the hardware simpler, colorless demodulation with different transmission distances starting from 200 km to above 6000 km had been used.

For the next generation transceiver, more and advanced features had been anticipated as the industry was moving forward into the future since 2014.

Firstly, the data rate per transceiver had been anticipated to touch at least in Tbps. And this is happening nowadays. Super-channel technology which is used nowadays in CO-OFDM(Coherent Optical Orthogonal Frequency Division Multiplexing) was once anticipated to be used for dealing with speed limitations of electronic devices[23].

Secondly, the flexibility and tunability in bandwidth and highly adaptable spectrally efficient system is now very important for sending a signal in flexi-grid optical network[24]. They sent signals in Tbps without any electronic digital-to-analog converters (DACs) [25].

Lastly, low power consuming and usable for any modulation format Digital Signal Processing was once anticipated to make hardware simpler and cost effective in today's generation transceivers.

It is now been anticipated by year 2030 physical limit of a single strand of optical SMF(Single Mode Fiber)will touch 100Tbps capacity.Then DSDM(Dense Space Division Multiplexing) & Hybrid Optical Switching(Optical (Circuit +Burst +Packet)Switching) may be able to tackle the high demand situation.

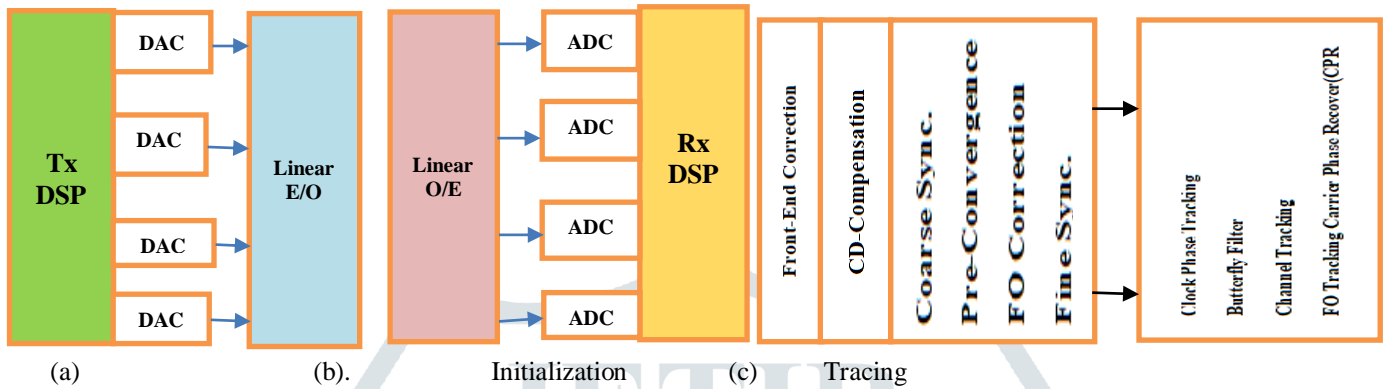


Figure: 25 Structure of (a)Flexible transmitter.(b)Receiver.(c)Proposed Receiver Side DSP,E/O,O/E,Synchronization.[38]

As described by them, Figures 17(a), (b) and (c) has transmitter, receiver, synchronization respectively. Transmitted binary signal sequence was encoded and then converted to analog signal by digital to analog converters(DACs). DSP did the changing of the modulation formats, tuning bit rates, pulse shaping, reducing chromatic dispersion and nonlinearities in fiber channel. Linear RF drivers, E/O(Electrical to Optical) converter were used for converting electrical signal to optical signal. In addition IQ modulators were important for high quality and high order QAM. After coherent demodulation at receiver optical signal was converted back to electrical signal using O/E(Optical to Electrical) converter. The electrical analog signal was converted back to digital signal using analog to digital converter(ADCs). Decoding was then done using DSP. And finally signal was received.

In their work, they had mentioned a DSP scheme as shown in Figure: 25 (c). It was simple, usable for any modulation format and well fit for parallel processing. It had two stages:-1)Initialization. 2)Tracing.

At first QPSK training symbols were sent for initialization. Where, two similar patterns each having 100 symbols were first passed through, for coarse synchronization using autocorrelation function of the transmitted training symbols. After that Constant Modulus Algorithm(CMA) did the pre-convergence of the butterfly filter.

Initial frequency offset(FO) estimation was done using those training symbols. Then chromatic dispersion(CD) was reduced(compensated). After that, fine synchronization was done using the cross-correlation between the received and transmitted training symbols [27]. Frequency offset drift was due to jitters in clock pulse, mechanical vibrations, polarization Mode Dispersion, rotation of a polarized signals and phase noise in lasers etc. Jitters in clock pulse was traced by square and filter method [26]

[The portion of this page is kept blank intentionally to make room for the figure.]

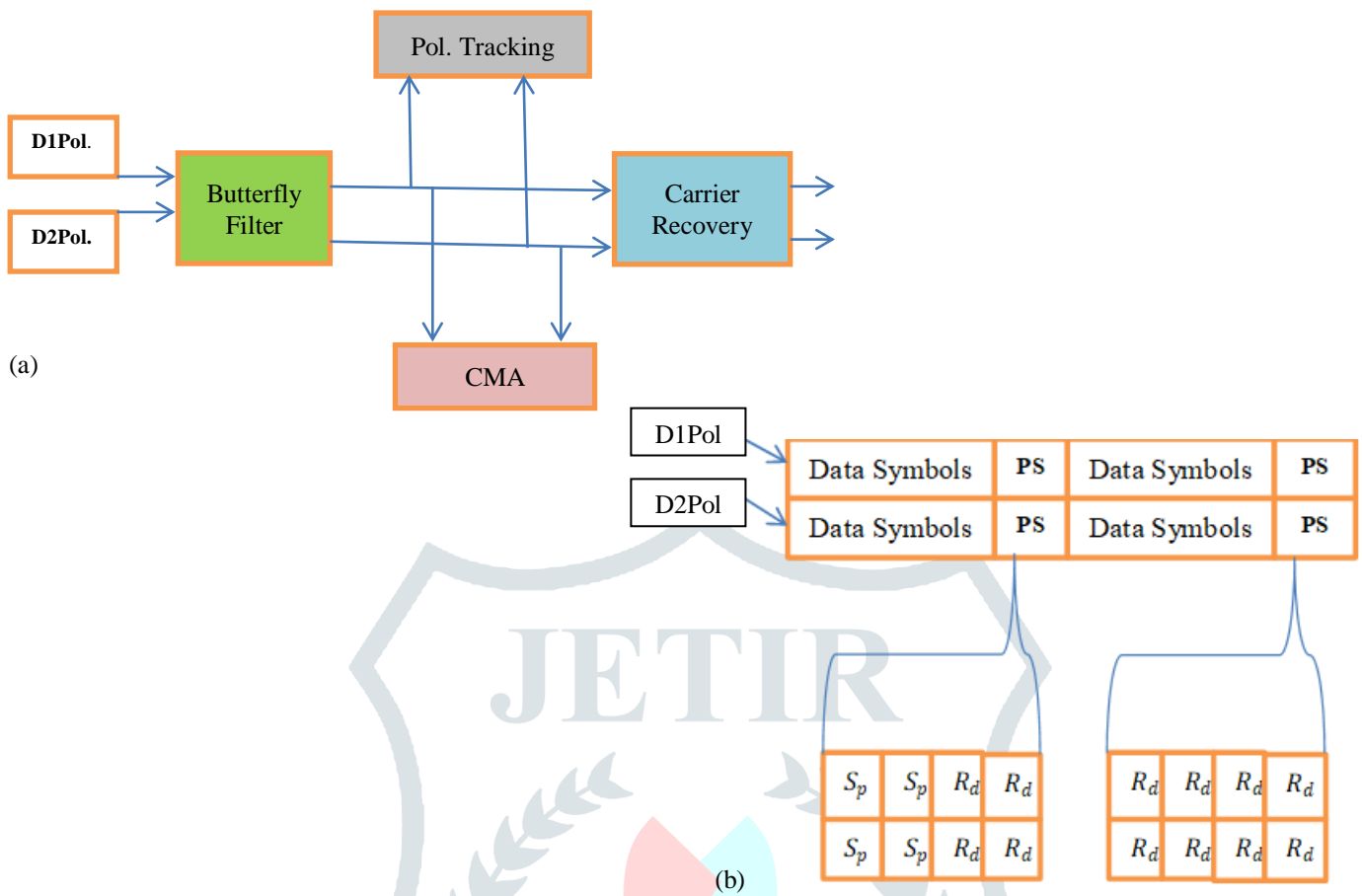


Figure: 26 (a)DSP structure. (b)Structure of a transmitted frame. S_p is special pilot symbol. R_d is random pilot symbol.[38]
(Pol = Polarization.)

Comparison and discussion

In their BER Vs FO drift rate plot, BER is near constant at lower FO drift (~0.1 to 1 MHz/ μ s). But at higher FO drift rate (~2 MHz/ μ s or more) BER increases drastically.

In their BER Vs polarization rotation drift rate plot, least mean square(LMS) data aided without differential coding had least and near constant BER. Also, it had least increasing rate for higher polarization rotation drift region. Pilot symbol aided CMA had largest BER increasing rate. However, with differential coding BER was increased and BER curve was shifted higher for data aided LMS.

Their simulation results was quite different from their real experimental results. And also, real experimental results was very much different from theoretical values which were a disadvantage. However, their proposed results for simulation and real experiment was nearly similar.

In their BER Vs OSNR plot, for simulation with differential coding LMS along with PLL had higher BER and decreasing rate of BER was slower for increasing OSNR relative to without differential coding. In that same plot, for real experiment, with and without differential coding LMS along with PLL BER curve was shifted to a higher BER region. Although with differential coding BER was still higher than without differential coding. In the same plot for 16,8 QAM and QPSK, QPSK had lowest BER and 16 QAM had highest BER and 8 QAM was intermediate. Although their BER was decreasing for increasing OSNR.

In their BER Vs distance plot, their proposed BER curve was close to without differential coding LMS,PLL and also lowest. However, with delay the same low level without differential coding LMs, PLL's BER curve shifted up with larger BER. In the same plot for 16,8 QAM and QPSK, QPSK with filter had lowest BER increasing for increasing distance. And 16 QAM colorless had highest BER increasing for increasing distance. 8 QAM was intermediate. Here, with or without(colorless) filter BER results for increasing distance in a particular modulation format was nearly same.

Also, in their BER Vs power plot, with differential coding LMS along with PLL, BER is highest even though it falls at lower power and then again increases for higher power. In the same plot for 16,8 QAM and QPSK, QPSK had highest BER but decreasing at faster rate at lower power region and lowest BER and nearly similar increasing rate with respect to 16,8 QAM at higher power region. 16 QAM even though had lowest BER and increasing rate of BER at lower power region was slowest but the BER was high and increasing rate was nearly similar with respect to 8 QAM and QPSK at higher power region. 8 QAM was intermediate.

Hence, it could be deduced from their plots that without differential coding LMS along with PLL, BER is always the lowest if no delays present and with differential coding it's highest. Also, QPSK systems have overall the best performance.

Spectrum of above mentioned three modulation format signals were plotted by them in normalized power Vs wavelength. QPSK had least power height but wider bandwidth, 16 QAM had highest power height and narrowest bandwidth. 8 QAM was as usual intermediate. Total power was similar, so power per wavelength bandwidth increased in higher order modulation formats.

In paper published in 2015 by Rodrigo Stange Tessinari, where they wrote, to reduce spectral occupancy (bandwidth) and to accommodate data traffic optical bandwidth was divided into spectrum units called frequency slices. ITU-T 694.1 standard declared granularity in frequency slot as 12.5 GHz so that 1,1.5,2THz optical bandwidth could have 80,120,160 frequency slices respectively. By varying the frequency slices spectrum variability could be achieved and spectral utilization could be improved. It had been a controversy and a hot topic whether moving to finer/smaller frequency slices (finer spectrum granularity) or even to a grid-less network operation may or may not be profitable much. Because additional cost to develop these modern technologies may or may not give desirable results that has higher network performance and cheaper cost simultaneously.

Flexible Single Carrier Transmission System:-

In order to reduce spectrum region used square power spectrum that had bandwidth matched baud rate was needed. Nyquist-shaped signal transmission was a modern technique used for this purpose. They used two equivalent transmitter for Nyquist-shaped single carrier Dual Polarization Phase Shift Keying (DP-PSK). It was dependent on digital and optical filter. Liquid Crystal on Silicon (LCoS) was used for making optical filter that had High Spectral Resolution (HSR). Signal's square like spectrum was somewhat smoothed using raised cosine filter near transmitter.

Therefore, total reserved spectrum after filtering was:-

$B.W_{Tx} = (1+\alpha).B.W$. where, α is roll-off factor. B.W is signal Band Width which was also the Baud Rate.

For smaller value of α rising and falling edge/skirt is sharper.

Figure: 27 below depicts various frequency slices (3.125 to 12.5 GHz).

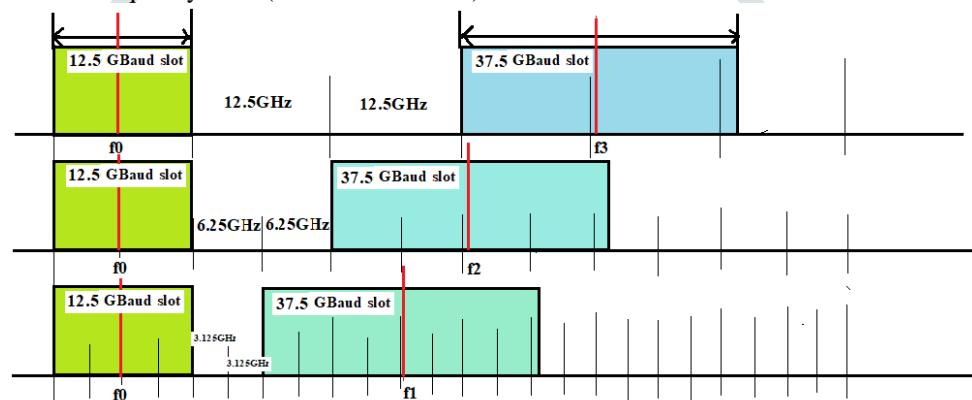


Figure:- 27 Giga Baud slots with different frequency slices (FS). f_1 , f_2 , f_3 , f_0 are central nominal frequencies. [40]

Comparison and discussion

It had been shown by them that as frequency slices (FS) size decreases the resolution is increased and resolution size decreases. And spectral penalty is least for lowest resolution (0.8 GHz) and with lowest Baud Rate (12.5 Gbaud). They also showed that smaller frequency slices (FS) had lesser Blocking Probability. For lower roll-off factor and lower resolution blocking probability is lower.

A tutorial on Flexible Optical network paradigm was written by Ioannis Tomkos, Siamak Azodolmolky, Josep Solé-Pareta, Davide Careglio, and Eleni Palkopoulou in 2013 where they mentioned, in fixed grid that was used in WDM systems, increasing subcarriers (channels) increases capacity but may decrease transparent reach. However by increasing channel spacing transparent reach could be increased to a certain extent. Also for maximum transparent reach an optimum launching power which was a constant value was required. But for multi bit rate/symbol rate, multi channel, multi modulation format system a constant launch power might lead to penalties. And making individual symbol rate channels with their respective optimum launch power system became impractical due to limitations at amplification stage. So, different transceivers required that had different costs and power consumptions. And that was a big issue. In fixed grid the channel spacing/frequency slices/grids were fixed to say 50 GHz or 100 GHz.

In flexi grid the frequency slot (bandwidth) could be varied which means bit rate could also be varied. The channel spacing/frequency slices/grids could be varied. Modulation format can also be varied which means flexi grid can be made modulation format transparent. Higher modulation formats can increase capacity, spectral efficiency as higher modulation formats has larger bits per symbol. In flexi grid bit rate can be switched automatically by flexible transponder and WSS (Wavelength Selective Switches). (WSS are made up of LCoS and MEMS). Flexi grid is mostly used in DWDM and more advance systems.

Set of nominal frequency f is given by:-

$f = 193.1 + (\pm n \times 6.25 \times 10^{-3})$ THz where, frequency slice/granularity is 6.25 GHz. 193.1 THz is anchor frequency also one of central nominal frequency.



Figure:28 two different slots.[40]

In a dynamic network when incoming connections were set up and disconnected in a random fashion spectrum resources tended to be immensely broken into pieces(fragmented) where unavoidable gaps were introduced in the spectrum. Breaking up of the spectrum resources due to this unavoidable gaps is called spectrum fragmentation.[28],[39],[57],[59],[60]

There are two types of fragmentation.[39]

(i) *Inter-link Fragmentation*:- It happens because of lack of continuity in frequency slots of different links.[39]

(ii) *Intra-link Fragmentation*:- It happens because of lack of contiguity(adjacency) in spectrum environment in same link.[39]

Fragmentation led to inefficient spectrum resource utilization. Ultimately this caused performance deterioration. Because unused frequency slices were scattering over whole spectrum range and contiguous(adjacent) frequency slots were not available for new connections Blocking Probability increased. So to combat this scenario various spectrum defragmentation techniques[39],[57] were introduced which are:-

- a) Re-optimization.
- b) Make-Before-Break(MBBR).
- c) Push-Pull defragmentation.[28]
- d) Optical Hop Tuning(Make-Before-Break+ Push-Pull defragmentation).[39]

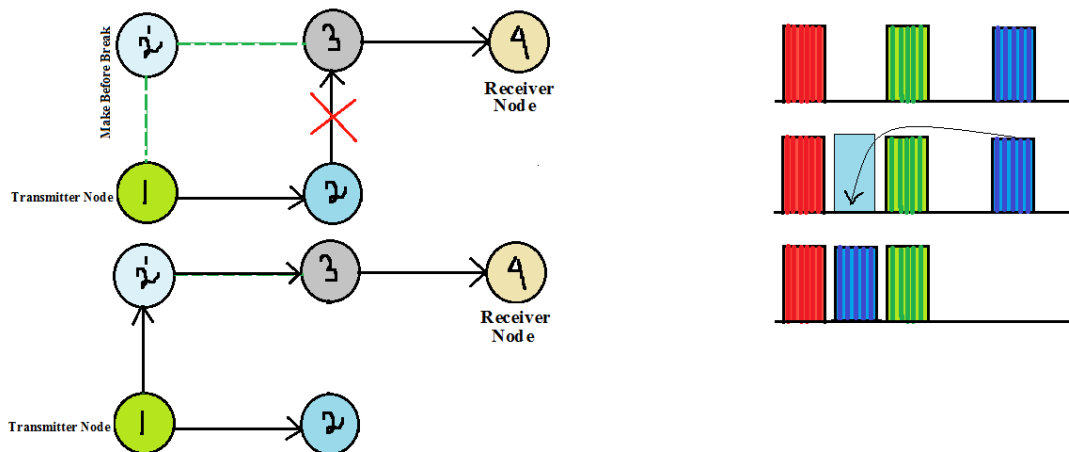


Figure: 29 MBBR.[39],[57]

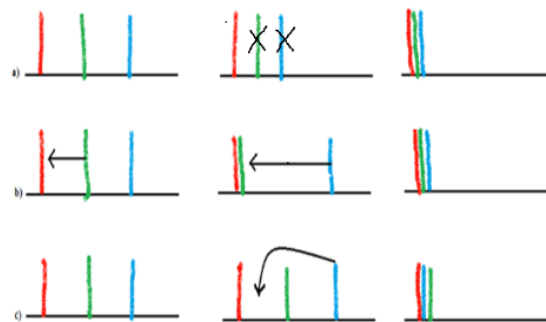


Figure:30 a)Re-optimization, b)push-pull defragmentation, c)Hop tuning.[39],[57]



Figure:31 Fixed grid Vs Flexi grid fiber.[58]

Comparison and discussion

In their plot of spectrum used Vs inter node traffic demand in Gbps both Electrical OFDM and Optical OFDM had used lowest spectrum for higher data rate. Although Electrical OFDM wins above all in terms of least spectrum usage and performance. And single line rate WDM system used the most spectrum as data traffic rate and demand was increasing and hence it had worst performance. Multi line rate WDM system used intermediate spectrum with increasing data traffic rate and demand. In their number of transponder Vs inter node traffic demand in Gbps plot Electrical OFDM, Optical OFDM and multi line rate WDM systems needed least transponders. Also, increasing rate of transponder requirements with increasing traffic demand and traffic data rate was lowest. While for single line rate WDM system number of transponders required was very high for increasing data traffic rate and demand. Optical Hop-tuning[39] may be the best that has twin benefits of MBBR and push-pull techniques but it needs costly optical devices.

In 2017 a work was done by ZhilinYuan, WeiLi,XiaopingWu, RuiYang, JinpingGuo, FanWang, LidanSong, QuianggaoHu, LipingSun,DequanXie, ZuoweiXuo where they wrote, the ROADM has been evolving along with the evolution of optical network(EON-Elastic Optical Network). They used two pairs of prisms. They first pass input light through a polarizer, one of the two prism pair, one of the two gating, one of two spherical lens and reflect the light using two mirrors held at some ninety degree angle. Then the light passed through second spherical lens on to a liquid crystal module and after that the light is reflected through lens, another gating, another pair of prisms, polarizer and came out as output pass band filtered light.

Comparison and discussion

Optical pass band filter with tunable bandwidth and wavelength was an important optical device in C/D/C/F(Colorless/Directionless/Contention less/Flexible) ROADM. To implement an optical filter multiple micro ring resonator, Mach Zender(MZ) interference effect etc were used. But they had narrow tunable bandwidth, poor temperature performance, large insertion loss. So, they proposed an optical pass band filter whose bandwidth was tunable in a wide range(50GHz to 500GHz), with insertion loss(<3dB) and with larger attenuation range.

In a work done by Zhi-shuShen, Hiroshi Hasegawa, Ken-ichi Sato, published in 2015, they mentioned, for providing future dynamic network services like optical layer protection and restoration, future flexible optical switch, enhancing agility and flexibility of OXCs had been a must. So, ROADM(also called C/D/C (Colorless/Directionless/Contention less))were required. Using Coherent OFDM, Nyquist WDM, distance adaptive modulation in flexi-grid network could maximize spectral efficiency, improved frequency utilization by 30% and reduced fiber cost compared to fixed-grid networks. However, spectrum fragmentation, blocking ratio inequality existed in fixed grid which needed to be overcome before using flexi-grid. Several defragmentation techniques had been used like, a)Re-optimization, b)MBBR, c)Push-Pull de-fragmentation, d)Hop Tuning to resolve spectrum fragmentation issue. Most defragmentation focuses on reduction of blocking of smaller bit rate channels and avoids the reduction of blocking of higher bit rate channels. Higher bit rate channels occupy wider frequency bandwidth. This inequality in dealing with blocking of different bit rate channels is called Blocking Ratio inequality which could deteriorate quality of signal. They used MBBR where dynamic re-routing minimizes traffic disruption and spectrum defragmentation along with blocking ratio inequality equalization techniques. In those techniques, exclusive contiguous(adjacent) frequency slot area for the highest bit rate channel was introduced for both flexi-grid and semi flexi-grid network. The MBBR(Make-before-break) set up re-routing alternate paths and assigned frequency slots before leaving previous paths. Thereby, it reduced disruption time. And the delay management technique that was also present using buffer memory made it a hitless re-routing. And Blocking Probability was reduced. In addition exclusive contiguous frequency slot are allocation for higher bit rate channel equalized the blocking ratio inequality.

Fixed-grid system:-

- Say three different bit rates 10,40,100 Gbps are accommodated on three different bandwidth slots that has fixed channel spacing/frequency slices/grids which is either 50GHz or 100GHz.
- Central nominal frequencies are fixed.

Flexi-grid system:-

- The channel spacing/frequency slices/grids are variable and can be lowered down to finer granularity of 3.125,6.25,12.5 GHz.
- Central nominal frequencies are fully flexible(variable).

Semi-Flexi grid systems:-

- a)The channel spacing/frequency slices/grids are semi flexible which means the frequency slots that has different bit rates and different bandwidths can be moved to a certain range within the slots.
- b)Central nominal frequencies are semi-flexible.

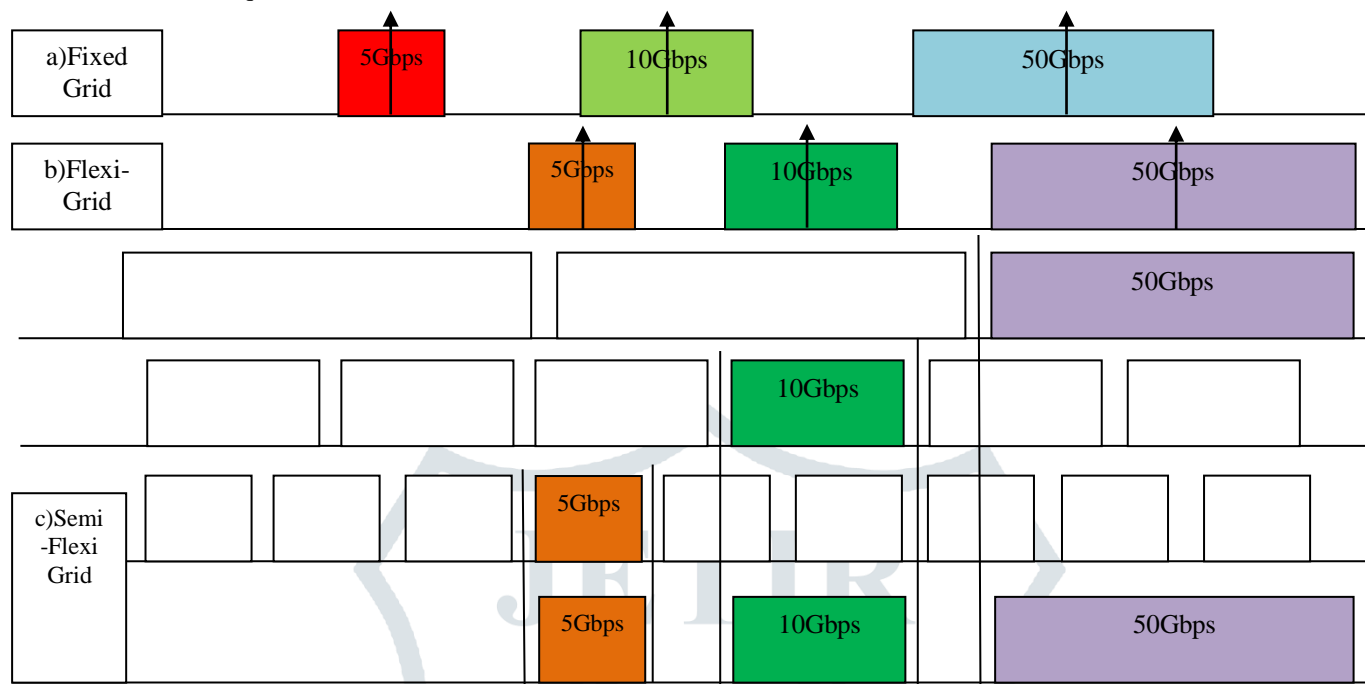


Figure: 32 a)Fixed-Grid, b)Flexi-Grid, c)Semi-Flexi Grid.[42]

Comparison and discussion

In their blocking ratio Vs traffic load plot for both flexi grid and semi flexi grid systems for various networks, Make before Break second method had the least and lowest increasing rate blocking ratio with increasing traffic load. And first fit method had the highest and greater increasing rate blocking ratio with increasing traffic load. Shannon entropy method also had higher blocking ratio than Make before Break second and first method but lower than first fit method.

A work has been done in[43]where it is described as, CO-OFDM(Coherent Optical Orthogonal Frequency Division Multiplexing) has Coherent Optical detection and Orthogonal Frequency Division Multiplexing which has the following advantages:-

- 1)Chromatic Dispersion(CD) and Polarization Mode Dispersion(PMD) can be found and reduced.
- 2)Since spectrum of OFDM sub-carriers are partially overlapped(like super channel) the optical spectral efficiency is very high.
- 3)Direct Up/Down conversion used here reduces bandwidth size significantly which is useful for high speed circuit design where signal bandwidth is costly.
- 4)Signal processing in OFDM can use FFT and IFFT algorithm efficiently. It means OFDM exhibits better scalability on channel dispersion as well as on variable data rate.

Introduction of virtual sub-carrier has following advantages:-

- 1)Prevents filtering range of OFDM signal being restricted as FO exist and that reduced high performance needs of filter.



Figure: 33 (a) Restricted fixed range for filtering. (b) Wider/stretched range for filtering.

2)Power given on virtual sub-carriers is ideally zero and these are not used to carry data.

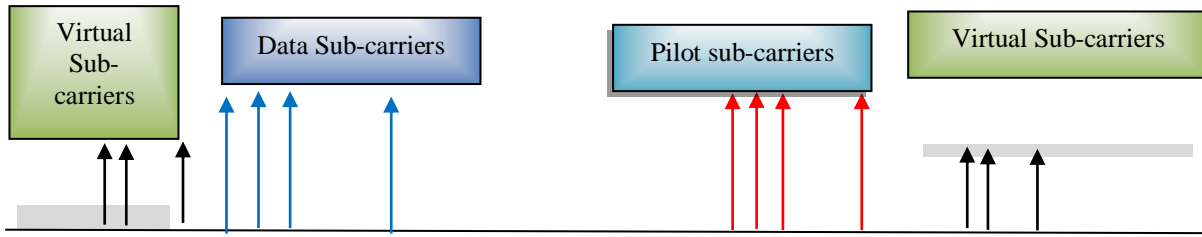


Figure: 34 Sub-carriers sequence.[43]

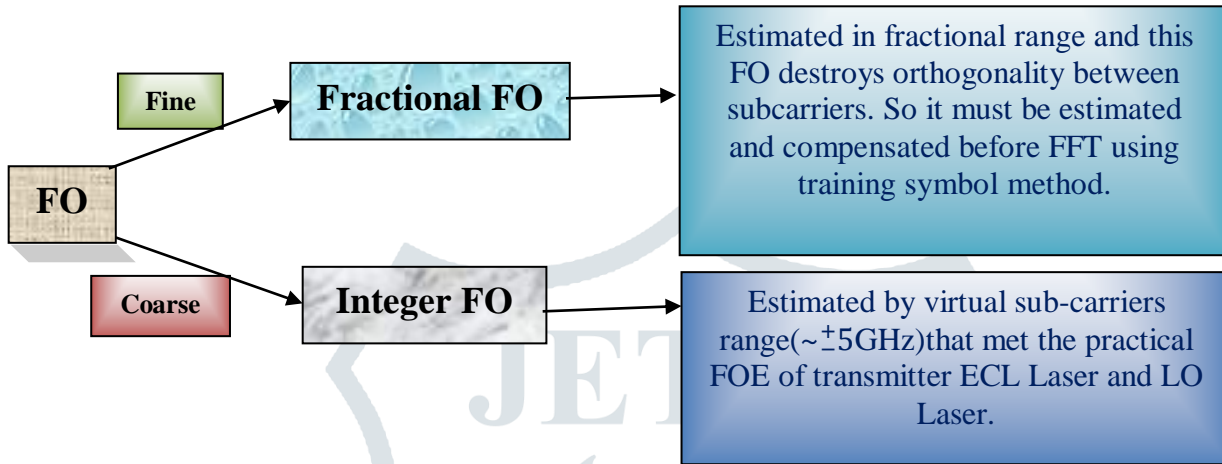


Figure: 35 Types of Frequency Offset(FO).[43]

Comparison and discussion

It is better than older Schmidh method of timing metric for MAP(Maximum-A-Posteriori) Estimation[16]. The CO-OFDM system is effected only by AWGN only. When carrier FO is 1GHz and OSNR is between 0-20dB range in AWGN channel, normalized MSE(Mean Square Estimation) is lowered with increasing OSNR with respect to older Smidth method. And it is independent of actual FO(i.e; MSE is almost constant for different FO).

In 2010 a work done by Yaojun Qiao , Zhansheng Wang, and Yuefeng Ji on blind frequency offset estimation by few authors is described below.

Problems of CO-OFDM:-

- 1)Sensitivity to synchronization errors and Frequency Offset(FO). As all sub-carriers are overlapped and orthogonal to each other a minor FO will lead to lose the orthogonality.
- 2)FO degrades system performance.
- 3)FO causes ICI(Inter Carrier Interference).

OFDM can eliminate ISI(Inter Symbol Interference) due to CP(Cyclic Prefix)which is a copy of the OFDM signal at the end and it's redundant in carrying data message.

Here, if $\Delta f_{estimation} range \approx \pm(\Delta f_{sub-carrier spacing})/2$ Frequency Offset Estimation accuracy is good but outside this range estimation accuracy decreases.

[The portion of this page is kept blank intentionally to make room for the figure.]

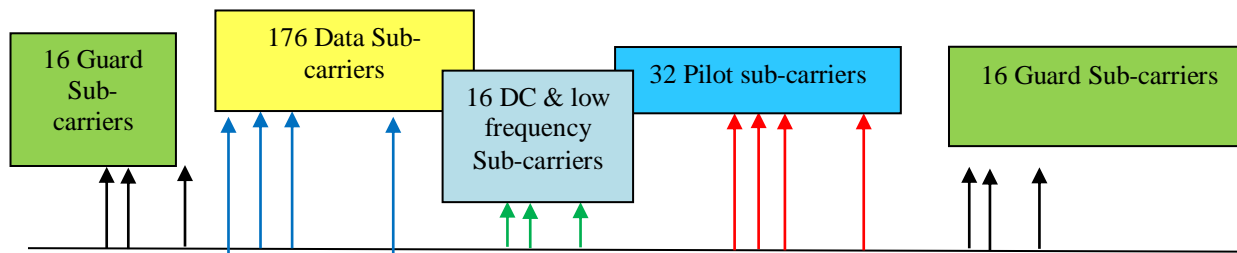


Figure: 36 Sub-carriers sequence.[44]

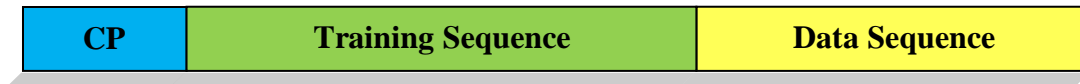


Figure: 37 Training and data sequence appended with Cyclic Prefix(CP).[44]

Blind FOE(Frequency Offset Estimation)[44] has three parts:-

- 1) Fractional FOE based on CP.
- 2) Integral FOE based on virtual sub-carriers.
- 3) Residual FO compensation based on pilots.

Comparison and discussion

Increasing CP length decreases Chromatic Dispersion and ISI.

As Chromatic Dispersion increases MSE increases. As OSNR increases MSE decreases slowly for longer length CP and MSE decreases faster for shorter length CP. But with variation of FO and with increment of FO, MSE doesn't change much.

Training Symbols:- It is a preset OFDM symbols known at receiver end. It helps receiver to trace and recover the time-invariant signal from distortions. It does that by using correlation function between receiver training symbols and transmitted training symbols.

Pilot symbols:- It is a certain orthogonal sub-carriers inserted in the OFDM symbol spectrum. It is used to estimate dynamic movement of neighboring sub-carriers.

III. SIMULATION DONE AT THE LAB

At first I took number of samples per bit, bit rate, number of bits as 64, 10Gbps and 1024 respectively. So total number of samples(N)=number of samples per bit(N_{spb})× number of bits(N_{of_bits})=64×1024=65,536. We know, bit duration(T_b) is inversely proportional to R_b i.e. ($T_b = \frac{1}{R_b}$) and sampling frequency(f_s) is equal to product of N_{spb} and bit rate(R_b). And so sampling time(t_s) is inversely proportional to sampling frequency(f_s) i.e. ($t_s = \frac{1}{f_s}$). I took length of frequency(F) scale to be f_s such that it stretches from $-\frac{f_s}{2}$ to $(\frac{f_s}{2} - \frac{f_s}{N})$ in steps of $\frac{f_s}{N}$ Hertz(Hz), and length of time(t) scale to be $N \cdot t_s$ such that it stretches from 0 to $t_s \cdot (N - 1)$ in steps of t_s . At the transmitter(Tx) end a random bit sequence is taken which could be generated in practical by a Bit Pattern Generator(BPG). That random bit sequence is rounded off to nearest integer. After saving and running the simulation, the pulse is thus generated with time Vs pulse amplitude after I added some noise which is random in nature. I put that pulse in a simulation window before plotting output and then labelled both x and y axes as time in seconds and amplitude respectively.

I got the spectrum magnitude plot after doing FFT(Fast Fourier Transform) followed by taking its magnitude. Then again I plot frequency(F) Vs magnitude spectrum of output noisy signal. In order to show the Frequency Offset(FO) at receiver(Rx) end signal, I mixed a variable with the received signal where f is FO which also a function of that variable. I used simulation window for plotting such that the pulse spectrum moves(shifts) smoothly. And then I labelled x and y axes as frequency(in Hertz) and magnitude.

After that I created a spectral window and took number of frequency samples per window as equal to window width(band) divided by step size of $\frac{f_s}{N}$ Hertz. Magnitude of shifted pulse spectrum also plotted. A window does the sum of all the peak power points along the frequency axis as the window band sweeps(also called Spectrum Scanning) according to FO. Plot was then labelled x and y axes as frequency(Hz) and window sum. I found maximum peak power. Also showed FO value. Lastly for auto filter position tracking a Gaussian function was used. Then I plot the Gaussian function on top of previous window sum plot such that the two figure moves together and changes width together. After that I created a simulation filter separately to filter some of the noise that was added during simulation. The block diagram of the simulation and the output plots are given below in figure: 38 and 39 respectively.

[The portion of this page is kept blank intentionally to make room for the figure.]

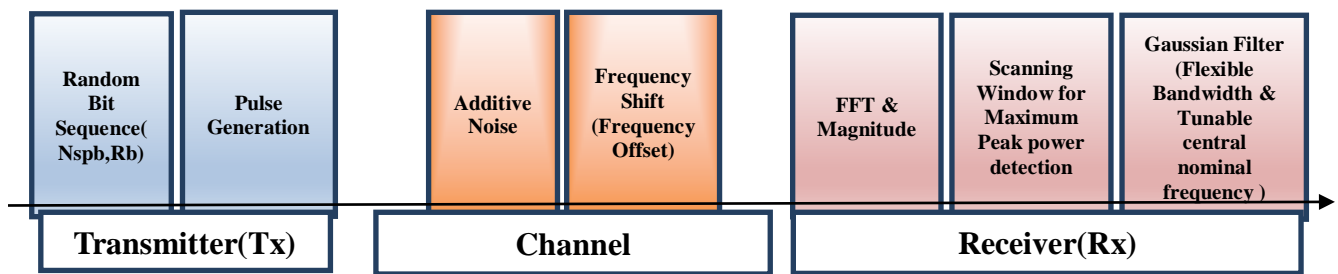


Figure: 38 Block diagram of simulation model.

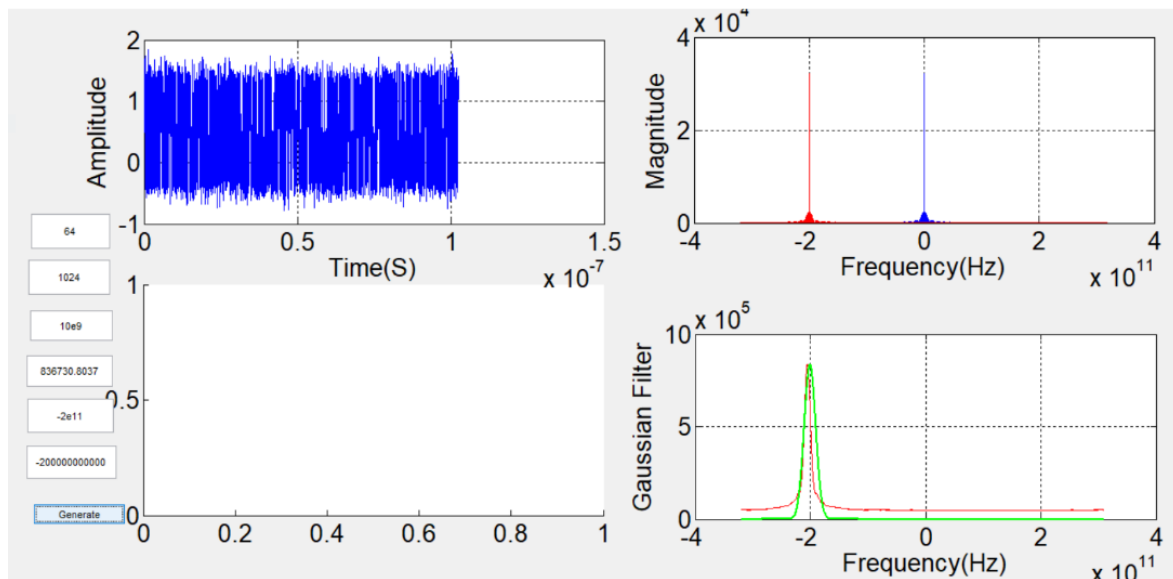


Figure:39 Plots of noisy random pulse, Magnitude Spectrum, Window Sum, FO in a received signal.

IV. FUTURE SCOPE

As the time's passing by and we are stepping into the next generation, there is a growing demand for higher data speed and more data quantity. To meet this requirements it is a necessity that the receiver for a communication system is very well equipped with the latest and upgraded new technologies where a filter is made intelligent enough to track the frequency drift, estimate frequency and phase offset and accordingly adjust it's central frequency and also reconfigure the essential bandwidth as per needed for any modulation format(i.e; format-transparent) and at any bit rate. Lately many work is going on developing the receiver and transmitter systems. I myself did simulation on MATLAB which is described above, for getting a flavor of tracking the frequency offset and placing a gaussian filter smartly and automatically for filtering the signal.

In future it is expected one could devise a receiver system where all these functions mentioned above are met thereby the data carrying capacity crunch and many other issues will be resolved.

From all the studies I have done, it can be anticipated by year 2030 physical limit of a single strand of optical SMF(Single Mode Fiber)will touch 100Tbps capacity[63],[69]. Above that bit rate limit, DSDM(Dense Space Division Multiplexing)[69]& Hybrid Optical Switching[66](Optical(Circuit +Burst +Packet)Switching) may be able to tackle the high demand situation.On adaptability[62]effective and higher bandwidth usage along with content preservation is a major factor in flexible optical systems. There could be any man made to natural calamities due to which optical link in the network may got broken leading to link failure. BCP's[62] K^{th} and Modified shortest path methods took care of the multi link failure due to any calamities, quite well. In case of content preservation during any calamity back up[62] and working path[62] needed to be in separate content node.To make a new connection, break old one, preserving connectivity even in immensely damaged links situation, etc. a request is required to be sent from source node. This node contains path information of how much bandwidth isrequired for setting up main path and back up path. Also this node looks for nearest path and the most unused path available.If enough spectrum regionis available then new paths are created. If not available then request is stopped. Also making the optical systems self-sustainable is a challenge, however self-sustainability[61] is a boon for the next generation optical communication.

Today, 26thDecember 2018 as I am typing this and now in this upcoming new year 2019, my hometown Agartala and other regions of Tripura is still now and it will be still facing then thedisruption in 4G connectivity.It happens that sometimes there is no internet for the whole day long.The data consumption requirement is lot more than the internet providers can provide in cheapest way. As we know wherever internet set foot educational institutions, society, industries, banking sectors and transportation

sectors started developing at faster rate. I suggest, with the coming 5G technology along with the implementation of flexible optical systems in my hometown and other regions for all users in vast scale, in cheapest and ecofriendly way would benefit us all. And this would benefit the country in some way, which would benefit the world ultimately.

V. CONCLUSION

Along with the ever growing demands of data capacity, data speed & reliability optical network has been evolving from 1st generation Optical Network that had fixed point to point DWDM links in core based ITU – Fixed grid system with ~50GHz frequency slots & 10Gbps OOK/BPSK modulation to Flexi grid system based on ITU G 694.1 with multi granularity in frequency slots(12.5GHz,6.25GHz,3.125GHz etc.), grid-less & with higher order modulation formats(M-PSK,M-QAM etc.)with variable bit rates, with OFDM, with higher spectral efficiency & higher bit rates. If a system is made such that it's spectrum region can automatically adjust itself by increasing and decreasing the bandwidths according to increasing and decreasing bit rates respectively and also there is shifting of central nominal frequencies(slots) according to variation of increment or decrement of number of channels in order to make room for extra channels in the spectrum region then a smart, adaptable, flexible and tunable optical system that has smart optical filters is definitely possible.

REFERENCES

- [1]P. Gianni, G. Corral-Briones, C. E. Rodriguez, H. S. Carrer, and M. R. Hueda, "A new parallel carrier recovery architecture for intradyne coherent optical receivers in the presence of laser frequency fluctuations," in Proc. IEEE GLOBECOM'11, pp. 1–6.
- [2]S.-H. Fan, J. Yu, D. Qian, and G.-K. Chang, "A fast and efficient frequency offset correction technique for coherent optical orthogonal frequency division multiplexing," *J. Lightwave Technol.* 29(13), 1997–2004 (2011).
- [3]X. Zhou, X. Chen, and K. Long, "Wide-range frequency offset estimation algorithm for optical coherent systems using training sequence," *IEEE Photon. Technol. Lett.* 24(1), 82–84 (2012).
- [4] E. Ip and J. M. Kahn, "Feedforward carrier recovery for coherent optical communications," *J. Lightwave Technol.* 25(9), 2675–2692 (2007).
- [5]T. Pfau, S. Hoffmann, and R. Noé, "Hardware-efficient coherent digital receiver concept with feedforward carrier recovery for M-QAM constellations," *J. Lightwave Technol.* 27(8), 989–999 (2009).
- [6]M. G. Taylor, "Phase estimation methods for optical coherent detection using digital signal processing," *J. Lightwave Technol.* 27(7), 901–914 (2009).
- [7] Q. Zhuge, M. Morsy-Osman, X. Xu, M. E. Mousa-Pasandi, M. Chagnon, Z. A. El-Sahn, and D. V. Plant, "Pilotaidd carrier phase recovery for M-QAM using superscalar parallelization based PLL," *Opt. Express* 20(17), 19599–19609 (2012).
- [8]U. Koc, A. Leven, Y. Chen, and N. Kaneda, "Digital coherent quadrature phase-shift-keying (QPSK)," in Proc. Opt. Fiber Conf. (OFC), Anaheim, CA, 2006, Paper OThI1.
- [9] D.-S.Ly-Gagnon,S.Tsukamoto,K.Katoh,andK.Kikuchi,"Coherent detection of optical quadrature phase-shift keying signals with carrier phase estimation," *J. Lightw. Technol.*, vol. 24, no. 1, pp. 12–21, Jan. 2006.
- [10]L. G. Kazovsky, "Phase- and polarization-diversity coherent optical techniques," *J. Lightw. Technol.*, vol. 7, no. 7, pp. 279–292, 1989.
- [11]P. S. Cho, G. Harston, C. J. Kerr, A. S. Greenblatt, A. Kaplan, Y. Achiam, and I. Shpantzer, "Coherent homodyne detection of BPSK signals using time-gated amplification and LiNbO₃ optical 90° hybrid," *IEEE Photon. Technol. Lett.*, vol. 16, no. 7, pp. 1727–1729, 2004.
- [12]C. Dorrer, C. R. Doerr, I. Kang, R. Ryf, J. Leuthold, and P. J. Winzer, "Measurement of eye diagrams and constellation diagrams of optical sources using linear optics and waveguide technology," *J. Lightw. Technol.*, vol. 23, no. 1, pp. 178–186, 2005.
- [13]D.-S.Ly-Gagnon,S.Tsukamoto,K.Katoh,andK.Kikuchi,"Coherent detection of optical quadrature phase-shift keying signals with carrier phase estimation," *J. Lightw. Technol.*, vol. 24, no. 1, pp. 12–21, 2006.
- [14]E. C. M. Pennings, R. J. Deri, R. Bhat, T. R. Haynes, and N. C. Andreadakis, "Ultra-compact, all-passive optical 90°-hybrid on InP using self-imaging," *IEEE Photon. Technol. Lett.*, vol. 5, no. 6, pp. 701–703, 1993.
- [15]R. Epworth, J. Whiteaway, and S. J. Savory, "3 Fibre I & Q Coupler," U.S. patent 6859586, 2005.
- [16]M. G. Taylor, "Phase estimation methods for optical coherent detection using digital signal processing," *J. Lightwave Technol.* 27(7), 901–914 (2009).
- [17] T. Pfau, S. Hoffmann, and R. Noe, "Hardware-efficient coherent digital receiver concept with feedforward carrier recovery for M-QAM constellations," *J. Lightwave Technol.* 27(8), 989–999 (2009).
- [18] E. Ip and J. M. Kahn, "Feedforward carrier recovery for coherent optical communications," *J. Lightwave Technol.* 25(9), 2675–2692 (2007).
- [19]I. Fatadin, D. Ives, and S. J. Savory, "Laser linewidth tolerance for 16-QAM coherent optical systems using QPSK partitioning," *IEEE Photon. Technol. Lett.* 22(9), 631–633 (2010).
- [20] Y. Gao, A. P. T. Lau, S. Yan, and C. Lu, "Low-complexity and phase noise tolerant carrier phase estimation for dual-polarization 16-QAM systems," *Opt. Express* 19(22), 21717–21729 (2011).
- [21]Q. Zhuge, M. E. Pasandi, X. Xu, B. Châtelain, Z. Pan, M. Osman, and D. V. Plant, "Linewidth-tolerant low complexity pilot-aided carrier phase recovery for M-QAM using superscalar parallelization," in Proc. OFC'12, Paper. OTu2G.2.
- [22] K. Piyawanno, M. Kuschnerov, B. Spinnler, and B. Lankl, "Low complexity carrier recovery for coherent QAM using superscalar parallelization," in Proc. ECOC'10, Paper. We.7.A.3.

- [23] S. Chandrasekhar and X. Liu, "Experimental investigation on the performance of closely spaced multi-carrier PDM-QPSK with digital coherent detection," *Opt. Express* 17(24), 21350–21361 (2009).
- [24] O. Gerstel, M. Jinno, A. Lord, and S. J. B. Yoo, "Elastic optical networking: a new dawn for the optical layer?" *IEEE Commun. Mag.* 50(2), s12–s20 (2012).
- [25] Y. Huang, E. Ip, P. N. Ji, Y. Shao, T. Wang, Y. Aono, Y. Yano, and T. Tajima, "Terabit/s optical superchannel with flexible modulation format for dynamic distance/route transmission," in *Proc. OFC'12*, Paper. OM3H.4 (2012).
- [26] M. Oerder and H. Meyr, "Digital filter and square timing recovery," *IEEE Trans. Commun.* 36(5), 605–612 (1988).
- [27] Q. Zhuge, M. Morsy-Osman, X. Xu, M. Chagnon, M. Qiu, and D. V. Plant, "Spectral efficiency-adaptive optical transmission using time domain hybrid QAM for agile optical networks," *J. Lightwave Technol.* 31(15), 2621–2628 (2013).
- [28] F. Cugini, F. Paolucci, G. Meloni, G. Berrettini, M. Secondini, F. Fresi, N. Sambo, L. Potì and P. Castoldi "Push-Pull Defragmentation Without Traffic Disruption in Flexi-Grid Optical Networks".
- [29] Tommaso Foggi, Giulio Colavolpe, Alberto Bononi, Paolo Serena "Spectral efficiency Optimization in Flexi-Grid Long-Haul Optical Systems".
- [30] Meng Qiu, Qunbi Zhuge, Xian Xu, Mathieu Chagnon, Mohamed Morsy-Osman, and David V. Plant "Simple and efficient frequency offset tracking and carrier phase recovery algorithms in single carrier transmission systems".
- [31] Xian Zhou, Xue Chen, and Keping Long "Wide Range Frequency Offset Estimation Algorithm for optical coherent systems using Training Sequence".
- [32] Koichi Ishihara, Tadao Nakagawa, Riichi Kudo, Munehiro Matsui, Takayuki Kobayashi, Yasushi Takatori, and Masato Mizoguchi NTT Network Innovation Laboratories, NTT Corporation, 1-1 Hikari-no-oka, Yokosuka, Kanagawa, 239-0847, Japan. "Wide-Range and Fast-Tracking Frequency Offset Estimator for Optical Coherent Receivers".
- [33] Pablo Gianni, Carmen E. Rodriguez, Graciela Corral-Briones, Mario R. Hueda and Hugo S. Carrer "A New Parallel Carrier Recovery Architecture for Intradyne Coherent Optical Receivers in the Presence of Laser Frequency Fluctuations".
- [34] Noriaki Kaneda, Andreas Leven, Ut-Va-Koc, Young-Kai-Chan all members of IEEE "Frequency Estimation in Intradyne Reception".
- [35] Joseph M. Kahn and Ezra Ip fellow members of IEEE "Feed Forward carrier recovery coherent optical communications".
- [36] Michael G. Taylor, "Phase Estimation Methods for Optical Coherent Detection Using Digital Signal Processing".
- [37] Qunbi Zhuge, Mohamed Morsy-Osman, Xian Xu, Mohammad E. Mousa-Pasandi, Mathieu Chagnon, Ziad A. El-Sahn, and David V. Plant, "Pilot-aided carrier phase recovery for M-QAM using superscalar parallelization based PLL".
- [38] Qunbi Zhuge, Mohamed Morsy-Osman, Mathieu Chagnon, Xian Xu, Meng Qiu, and David V. Plant, "Terabit bandwidth-adaptive transmission using low-complexity format-transparent digital signal processing".
- [39] RODRIGO STANGE TESSINARI, Supervisor: Prof. Dr. Anilton Salles Garcia, "A Fairness-Focused Spectrum Assignment Algorithm For Elastic Optical Networks by" Universidade Federal do Espírito Santo – UFES, Vitória-ES 2016. P-10,11,12,13.
- [40] "Investigation of spectrum granularity for performance optimization of flexible Nyquist WDM based optical networks" Pouria Sayyad Khodashenas, José Manuel Rivas-Moscato, Behnam Shariati, Student Member, IEEE, Dan M. Marom, Senior Member, IEEE, Fellow, OSA, Dimitrios Klonidis, and Ioannis Tomkos, Senior Member, IEEE, Fellow, OSA.
- [41] Zhilin Yuan, Wei Li, Xiaoping Wu, Rui Yang, Jinping Guo, Fan Wang, Lidan Song, Qiang Gao, Hu Liping Sun, Dequan Xie, Zuwei Xu, "Bandwidth and wavelength tunable optical passband filter with tunable attenuation based on transmission Liquid Crystal technology".
- [42] Zhi-shu Shen, Hiroshi Hasegawa, Ken-ichi Sato, "Integrity enhancement of Flexible/Semi-Flexible Grid networks that minimizes disruption in spectrum defragmentation and bitrate dependent blocking".
- [43] Jianfei Liu, Huimin Shi, Xiangye Zeng, Jia Lu, Mengjun Wang, Beilei Liu, "A Joint Frequency Offset Estimation Algorithm Based on Training Symbol and Virtual Subcarriers for CO-OFDM Systems".
- [44] Yaojun Qiao, Zhansheng Wang, and Yuefeng Ji, "Blind frequency offset estimation based on cyclic prefix and virtual subcarriers in CO-OFDM system".
- [45] "Optical Fiber Communication" by Gerd Keiser, P-453, 607.
- [46] J. M. Fabrega, M. Svaluto Moreolo, L. Martín, A. Chiadò Piat, E. Riccardi, D. Roccatò, N. Sambo, F. Cugini, L. Potì, S. Yan, E. Hugues-Salas, D. Simeonidou, M. Gunkel, R. Palmer, S. Fedderwitz, D. Rafique, T. Rahman, Huug de Waardt, A. Napoli, "On the Filter Narrowing Issues in Elastic Optical Networks".
- [47] "Communication Systems" by Simon Haykin. P-585.
- [48] Oleg V. Sinkin, Ronald Holzlöhner, John Zweck, and Curtis R. Menyuk, "Optimization of the Split-step Fourier Method in Modeling Optical Fiber Communications Systems", August 7, 2002.
- [49] Marco Secondini, Member, IEEE, Tommaso Foggi, Francesco Fresi, Gianluca Meloni, Fabio Cavaliere, Member, IEEE, Giulio Colavolpe, Senior Member, IEEE, Enrico Forestieri, Member, IEEE, Luca Potì, Member, IEEE, Roberto Sabella, Senior Member, IEEE, and Giancarlo Prati, Fellow, IEEE, "Optical Time-Frequency Packing: Principles, Design, Implementation, and Experimental Demonstration".
- [50] Neda Rezaei Malek, "Optimization of the Viterbi and Viterbi Carrier Phase Error Detection Algorithm" Department of Electrical Engineering Research and Science Campus, Islamic Azad University Tehran, Iran.
- [51] S. Norimatsu and K. Iwashita, "Linewidth requirements for optical synchronous detection systems with nonnegligible loop delay time," *J. Lightw. Technol.*, vol. 10, no. 3, pp. 341–349, Mar. 1992.
- [52] L. Li, Z. Tao, T. Hoshida, and J. C. Rasmussen, "Carrier synchronization in 43 Gbit/s coherent QPSK receiver," presented at the OECC 2007 Conf., Yokohama, Japan, Jul., Paper 12B1.

- [53]Jilong Han, Wei Li, Zhilin Yuan, Yansheng Zheng, and Qianggao Hu, “A Simplified Implementation Method of Mth-power for Frequency Offset Estimation”.
- [54]N. Noels, Student Member, H. Steendam, Member, M. Moeneclaey, Fellow IEEE, and H. Bruneel, “Carrier Phase and Frequency Estimation for Pilot-Symbol Assisted Transmission: Bounds and Algorithms”.
- [55]Weiner process concept is in the link, https://en.m.wikipedia.org/wiki/Wiener_process
- [56]Simon Haykin, “Communication Systems”. P-349,354.
- [57]Ioannis Tomkos, Siamak Azodolmolky, Josep Solé-Pareta, Davide Careglio, and Eleni Palkopoulou, “A Tutorial on the Flexible Optical Networking Paradigm: State-of-the-Art, Trends, and Research Challenges”.
- [58]Lucas R. Costa, Guilherme N. Ramos, André C. Drummond, “Leveraging adaptive modulation with multi-hop routing in elastic optical networks” Department of Computer Science, University of Brasilia (UnB), Brasilia, Brazil.
- [59]Defragmentation concept is at link,<https://en.wikipedia.org/wiki/Defragmentation>
- [60]F. Cugini, M. Secondini, N. Sambo, G. Bottari, G. Bruno, P. Iovanna, and P. Castoldi, “Push-pull technique for defragmentation in flexible optical networks,” in Proc. OFC/NFOEC Conf., Mar. 2012.
- [61]ADVA Optical Networking-Sustainability report 2017 is at Link, <https://www.advaoptical.com/en/about-us/sustainability>
- [62]Chen Ma, Jie Zhang, Yongli Zhao, Zilian Jin, Yachao Shi, Yang Wang, Meng Yin, “Bandwidth-adaptability protection with content connectivity against disaster in elastic optical datacenter networks”.
- [63]Yutaka Miyamoto, Hirokazu Takenouchi, “Dense Space-division-multiplexing Optical Communications Technology for Petabit-per-second Class Transmission” in link, <https://www.ntt-review.jp/archive/ntttechnical.php?contents=ntr201412ra3.html>
- [64]ITU-T G.694.1 TELECOMMUNICATION STANDARDIZATION SECTOR OF ITU (02/2012) SERIES G: TRANSMISSION SYSTEMS AND MEDIA, DIGITAL SYSTEMS AND NETWORKS Transmission media and optical systems characteristics – Characteristics of optical systems Spectral grids for WDM applications: DWDM frequency grid link, <https://www.itu.int/rec/T-REC-G.694.1-201202-1>
- [65]Pouria Sayyad Khodashenas, Advisor: Dr. Jaume Comellas Colomé, Co-advisor: Dr. Jordi Perelló Muntan, “Dynamic Routing and Spectrum Allocation in Elastic Optical Networks” Universitat Politècnica de Catalunya (UPC), Departament de Teoria del Senyal i Comunicacions (TSC), Academic year 2014-2015
- [66]Matteo Fiorani and Maurizio Casoni, “Hybrid Optical Switching Network and Power Consumption in Optical Networks” Department of Information Engineering University of Modena and Reggio Emilia Via Vignolese 905, Modena, Italy Slavisa Aleksic Institute of Telecommunications Vienna University of Technology Favoritenstrasse 9-11/389, Vienna, Austria.
- [67]M ARCIN M ARKOWSKI, “SPECTRUM FRAGMENTATION-AWARE STRATEGIES FOR DEADLINE-DRIVEN DYNAMIC MULTICAST SCHEDULING PROBLEM IN EON” Department of Systems and Computer Networks, Faculty of Electronics, Wrocław University of Science and Technology, Wyb. Wyspińskiego 27, 50-370 Wrocław, Poland
- [69]Takayuki Mizuno, Yutaka Miyamoto, “High-capacity dense space division multiplexing transmission” NTT Network Innovation Laboratories, NTT Corporation, Japan.
- [70]Pouria Sayyad Khodashenas, José Manuel Rivas-Moscoso, Behnam Shariati, Student Member, IEEE, Dan M. Marom, Senior Member, IEEE, Fellow, “Investigation of Spectrum Granularity for Performance Optimization of Flexible Nyquist-WDM-Based Optical Networks” OSA, Dimitrios Klionidis, and Ioannis Tomkos, Senior Member, IEEE, Fellow, OSA.
- [71]L. A. Al-Mayahi, A. Y. Fattah, “BIT RATE AND LOSSES LIMITATIONS IN SINGLE MODE FIBER”, Electrical and Electronic Department, University of Technology/ Baghdad/ Iraq.